Pediatrics and Neonatology (2014) 55, 412–413

Available online at www.sciencedirect.com

ScienceDirect

journal homepage: http://www.pediatr-neonatol.com

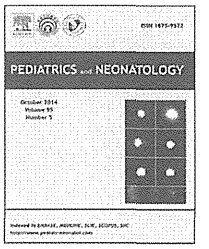

BRIEF COMMUNICATION

Tachyarrhythmia-induced Cerebral Sinovenous Thrombosis in a Neonate Without Cardiac Malformation

Wakato Matsuoka [a], Kenichiro Yamamura [a,*], Kiyoshi Uike [a], Hazumu Nagata [a], Shouichi Ohga [b], Toshiro Hara [a]

[a] *Department of Pediatrics, Graduate School of Medical Sciences, Kyushu University, Fukuoka, Japan*
[b] *Department of Perinatal and Pediatric Medicine, Graduate School of Medical Sciences, Kyushu University, Fukuoka, Japan*

Received Nov 19, 2013; received in revised form Jan 26, 2014; accepted Feb 5, 2014
Available online 28 May 2014

Neonatal cerebral sinovenous thrombosis (CSVT) is becoming increasingly diagnosed because of greater clinical awareness and improved neuroimaging techniques.[1,2] Despite the substantial mortality and morbidity, the etiology of pediatric CSVT has not been fully understood.[3] We herein report a case of 13-day-old infant who developed intractable paroxysmal supraventricular tachycardia, which was subsequently complicated with CSVT.

A 13-day-old Japanese male was admitted to our affiliated hospital because of poor feeding and not doing well for 2 days. The infant was delivered at term with a birth weight of 3458 g and full APGAR scores. There was no cardiomyopathy or prothrombotic disorder in his relatives. On admission, he presented tachycardia at 300 beats/minute with hypotension. The electrocardiogram (ECG) showed narrow QRS tachycardia with following P wave suggesting the diagnosis of paroxysmal supraventricular tachycardia (Supplementary Figure 1). Cardioversion (0.5 J/kg twice) after the intubation allowed restoration of a sinus rhythm. The patient was then transferred to our hospital for intensive treatment.

Initial physical examination demonstrated an afebrile and pale infant. He had a sinus rhythm but presented cold extremities and prolonged capillary refill time (>3 seconds). Auscultation revealed a gallop rhythm of the heart. Chest X-ray examination demonstrated pulmonary congestion and cardiac dilatation with a cardiothoracic ratio of 61%. The echocardiogram demonstrated an impaired left ventricular function with ejection fraction at the level of 50%. Laboratory examinations are as follows: white blood cell count 10.68×10^9/L; hematocrit 35.7%; platelet count 157×10^9/L; creatinine kinase 342 U/L; creatine kinase-MB 71 U/L; lactate dehydrogenase 601 U/L; C-reactive protein 0.11 mg/dL; troponin-T 0.154 ng/mL; prothrombin time—international normalized ratio 1.62; activated partial thromboplastin time 40.1 seconds; fibrinogen degradation products 63.1 μg/ml; D-dimer 28.5 μg/mL; and brain natriuretic peptide 3956 pg/mL.

The ECG during tachycardia documented the characteristics of atrioventricular reentrant tachycardia at 300 beats/minute. The tachycardia was terminated by the intravenous rapid infusion of ATP three times. The ECG during sinus rhythm showed no delta wave, suggesting the possibility of concealed WPW syndrome. Oral propranolol (1–2 mg/kg/day) and flecainide (3–6 mg/kg/day) succeeded to prevent the recurrence of refractory arrhythmia. The echocardiogram showed a smooth recovery of the left ventricular function to the normal level of 63% 2 days after admission.

* Corresponding author. Department of Pediatrics, Graduate School of Medical Sciences, Kyushu University, 3-1-1, Maidashi, Higashi-ku, Fukuoka 812-8582, Japan.
E-mail address: yamamura@pediatr.med.kyushu-u.ac.jp (K. Yamamura).

http://dx.doi.org/10.1016/j.pedneo.2014.02.003
1875-9572/Copyright © 2014, Taiwan Pediatric Association. Published by Elsevier Taiwan LLC. All rights reserved.

Author's personal copy

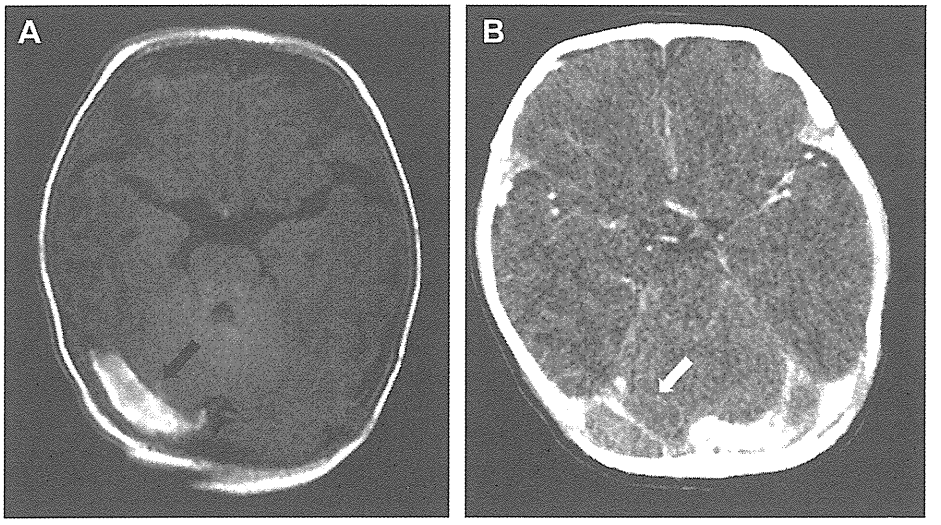

Figure 1 (A) T1-weighted magnetic resonance imaging. (B) Contrast-enhanced computed tomography of the brain after restoration of sinus rhythm. High signal intensity on T1-weighted magnetic resonance imaging (arrow) and flow disturbance on computed tomography (white arrow) confirmed the diagnosis of right transverse sinus thrombosis.

Magnetic resonance imaging (MRI) was performed 9 days after admission, in order to assess the cerebral damage due to cardiogenic shock. CSVT was indicated on MRI findings (Figure 1A). Computed tomography (CT) of the brain determined a right transverse sinus thrombosis (Figure 1B). Continuous infusion of fractionated heparin (10—22 unit/kg/hour, activated partial thromboplastin time 42—50 seconds) was started. Two weeks after the anticoagulant therapy, CT demonstrated recanalization of the transverse sinus. There were no laboratory data indicating inherited or acquired thrombophilic predispositions (on 12 days after admission): normal plasma activity of protein C 69%, protein S 58% and antithrombin 91%, and undetectable titer of anticardiolipin antibody 2 U/mL. The patient received no additional anticoagulant therapy. CSVT did not recur for 6 months after the first event.

This is the first report of neonatal CSVT as a complication of paroxysmal supraventricular tachycardia. Perinatal complications, dehydration, sepsis, meningitis, and inherited thrombophilias such as antithrombin, protein C, or protein S deficiency are the major associations with pediatric CSVT.[4,5] A recent case series reported that none of the neonates with CSVT had persistently low activity of protein C, protein S, or antithrombin, and some of them were considered to have acquired prothrombotic states.[4] This patient showed no evidence of prothrombotic disorders, although FD fibrinogen degradation products P and D-dimer had already been elevated on admission. Pediatric venous thrombosis occurs at the highest incidence in neonates. Extremely high brain natriuretic peptide level suggested the presence of cardiac deterioration due to prolonged tachycardia. We speculate that the cardiogenic shock led to the stasis of cerebral sinus venous flow that predisposed the neonate to developing thrombosis.

No randomized clinical trials have been conducted concerning anticoagulation therapy for neonatal CSVT. However, the American College of Chest Physicians recommended initial anticoagulation except in the presence of significant hemorrhage.[6] The favorable response to the short-term anticoagulant therapy in the present case might corroborate that CSVT was not associated with inherited coagulopathy, but the transient circulatory disturbance.

Because the symptoms of CSVT are nonspecific, and often subtle or asymptomatic, the diagnosis is delayed and may be missed altogether. Our patient did not present any neurological symptom at the diagnosis of CSVT. Intensive imaging tests including brain echogram, CT, and MRI, and appropriate anticoagulant therapy should be considered for the neonates having sustained tachyarrhythmia with cardiac failure.

Conflicts of interest

All contributing authors declare no conflicts of interest.

References

1. Heller C, Heinecke A, Junker R, Knöfler R, Kosch A, Kurnik K, et al. Cerebral venous thrombosis in children: a multifactorial origin. *Circulation* 2003;**108**:1362—7.
2. Wasay M, Bakshi R, Bobustuc G, Kojan S, Sheikh Z, Dai A, et al. Cerebral venous thrombosis: analysis of a multicenter cohort from the United States. *J Stroke Cerebrovasc Dis* 2008;**17**:49—54.
3. Berfelo FJ, Kersbergen KJ, van Ommen CH, Govaert P, van Straaten HL, Poll-The BT, et al. Neonatal cerebral sinovenous thrombosis from symptom to outcome. *Stroke* 2010;**41**: 1382—8.
4. Fitzgerald KC, Williams LS, Garg BP, Carvalho KS, Golomb MR. Cerebral sinovenous thrombosis in the neonate. *Arch Neurol* 2006;**63**:405—9.
5. Saracco P, Parodi E, Fabris C, Cecinati V, Molinari AC, Giordano P. Management and investigation of neonatal thromboembolic events: genetic and acquired risk factors. *Thromb Res* 2009;**123**:805—9.
6. Monagle P, Chalmers E, Chan A, DeVeber G, Kirkham F, Massicotte P, et al. Antithrombotic therapy in neonates and children: American College of Chest Physicians Evidence-Based Clinical Practice Guidelines (8th Edition). *Chest* 2008;**133**: 887S—968S.

Rheumatology Advance Access published May 11, 2014
RHEUMATOLOGY

Concise report

doi:10.1093/rheumatology/keu180

Early progression of atherosclerosis in children with chronic infantile neurological cutaneous and articular syndrome

Kenichiro Yamamura[1], Hidetoshi Takada[1], Kiyoshi Uike[1], Yasutaka Nakashima[1], Yuichiro Hirata[1], Hazumu Nagata[1], Tomohito Takimoto[1], Masataka Ishimura[1], Eiji Morihana[1], Shouichi Ohga[2] and Toshiro Hara[1]

Abstract

Objective. Chronic inflammation plays a key role in the development of atherosclerosis. Early progression of atherosclerosis has been reported in patients with RA. Cryopyrin-associated periodic syndromes (CAPS) are autosomal dominant autoinflammatory disorders caused by heterozygous *NLRP3* gene mutations. Chronic infantile neurological cutaneous and articular (CINCA) syndrome is the most severe form of CAPS and patients display early onset of rash, fever, uveitis and joint manifestations. However, there has been no previous report on atherosclerosis in patients with CAPS. The objective of this study is to assess the development of atherosclerosis in patients with CINCA syndrome.

Methods. Intima–media thickness (IMT) of the carotid arteries, stiffness parameter β, ankle brachial index (ABI) and pressure wave velocity (PWV) were evaluated by ultrasonography in 3 patients with CINCA syndrome [mean age 9.0 years (S.D. 5.3)] and 19 age-matched healthy controls [9.3 years (S.D. 4.3)].

Results. The levels of carotid IMT, stiffness parameter β and PWV in CINCA syndrome patients were significantly higher than those in healthy controls [0.51 mm (S.D. 0.05) *vs* 0.44 (0.04), $P = 0.0021$; 6.1 (S.D. 1.7) *vs* 3.9 (1.0), $P = 0.0018$; 1203 cm/s (S.D. 328) *vs* 855 (114), $P = 0.017$, respectively].

Conclusion. Patients with CINCA syndrome showed signs of atherosclerosis from their early childhood. The results of this study emphasize the importance of chronic inflammation in the development of atherosclerosis. Further analysis on atherosclerosis in young patients with CINCA syndrome may provide more insights into the pathogenesis of cardiovascular disease.

Key words: ankle-brachial index, atherosclerosis, chronic infantile neurologic cutaneous and articular syndrome, cryopyrin-associated periodic syndromes, intima-media thickness, pulse wave velocity.

CLINICAL

Introduction

It is well known that chronic inflammation is a predisposing factor for atherosclerosis. There has been considerable interest regarding the possible causal role of inflammation in the development of atherosclerosis in adult patients with RA, SLE and familial Mediterranean fever (FMF). Patients with SLE, APS or RA have increased mortality rates related to early atherosclerosis. Relative risk of 5 for myocardial infarction, 6–10 for stroke in SLE patients and 3.6 for cardiovascular deaths in RA patients has been reported [1]. Furthermore, the American Heart Association has reported that chronic inflammatory disease is one of the eight high-risk factors for atherosclerosis, even in children [2].

Cryopyrin-associated periodic syndromes (CAPS), including chronic infantile neurological cutaneous and articular (CINCA) syndrome, Muckle–Wells syndrome and familial cold autoinflammatory syndrome, are autosomal dominant autoinflammatory syndromes caused by heterozygous mutations of the *NLR family pyrin domain*

[1]Department of Pediatrics and [2]Department of Perinatal and Pediatric Medicine, Graduate School of Medical Sciences, Kyushu University, Fukuoka, Japan.

Submitted 25 November 2013; revised version accepted 11 March 2014.

Correspondence to: Kenichiro Yamamura, Department of Pediatrics, Graduate School of Medical Sciences, Kyushu University, 3-1-1, Maidashi, Higashi-ku, Fukuoka 812-8582 Japan.
E-mail: yamamura@pediatr.med.kyushu-u.ac.jp

© The Author 2014. Published by Oxford University Press on behalf of th
or Permissions, please email: journals.permissions@oup.com

containing 3 (*NLRP3*) gene. It has been reported that disease associated *NLRP3* mutation causes IL-1β oversecretion by caspase-1 activation. CINCA syndrome, the most severe form among them, is characterized by chronic systemic inflammation manifested as early onset of rash, fever, uveitis, chronic meningitis and joint symptoms [3]. However, there has been no previous report evaluating atherosclerosis in patients with CAPS.

Several physiological examinations are applied to assess atherosclerosis. Carotid intima–media thickness (cIMT) is known to be an indicator of atherosclerosis for adults and children [4]. In fact, increased cIMT has been shown in children with obesity, hyperlipidaemia and diabetes mellitus [5]. It has been reported that stiffness parameter β is more useful in detecting atherosclerotic changes in earlier stages than cIMT [6]. Also, pulse wave velocity (PWV) and ankle–brachial index (ABI) are simplified parameters of the severity of atherosclerosis and predictors of prognosis in adult patients with cardiovascular disease [7, 8]. The objective of this study is to assess the development and progression of atherosclerosis in young patients with CINCA syndrome by measuring cIMT, stiffness parameter β, PWV and ABI.

Patients and methods

Study population

Three patients (a 5-year-old boy [9], a 7-year-old girl [10] and a 15-year-old boy [11]) with CINCA syndrome and 19 age-matched healthy controls were enrolled in this study. *NLRP3* mutations were observed in all three patients. The parameters of atherosclerosis were investigated in these three patients who were in remission for 1 year after the initiation of canakinumab treatment. The Institutional Review Board of Kyushu University Hospital approved the study and informed consent was obtained from each subject.

Sonographic study

Carotid artery US was performed with an iE33 ultrasound machine (Philips, Amsterdam, The Netherlands) using an 11 MHz probe. Measurements were obtained with subjects in the supine position by experienced sonographers blinded to the subjects' clinical status. Ultrasonographic images of the right and left common carotid arteries (CCAs) of each subject at the lower third cervical region proximally and 1 cm above the carotid bulb distally in the longitudinal plane were obtained. CCA IMT measurements of the distal CCA posterior wall were done manually by the distance measurement system of the sonography device after magnification of the images. Three measurements were made in a non-neighbouring fashion within an ~1 cm segment from both the left and right CCA proximal and distal portions. The IMT was measured during end diastole. Mean IMT was calculated as the average of three consecutive measurements of maximum far wall thickness obtained from the CCA. Measurement of the internal diameter of the CCA was performed for three consecutive heartbeats. Intraobserver variability was 1.7% for IMT and 3.1% for arterial wall diameter measurements. The stiffness parameter β was calculated from this formula [12]: $\beta = [\ln(SBP/DBP)]/(\Delta D/D)$, where SBP is the systolic blood pressure, DBP is the diastolic blood pressure, D is carotid artery diastolic diameter and ΔD is the change in artery diameter during systole.

PWV and ABI

PWV and ABI were measured using a BP-203RPEIII (Omron Colin, Tokyo, Japan). PWV, ABI, the blood pressure of the extremities, ECG and heart sounds were synchronously measured and then automatically recorded. Electrodes were contacted on both wrists and a microphone was attached to the left margin of the sternum. The extremities were then wrapped by cuffs that were connected to a pulse monitor. The volume wave and time difference emitted from the pulse monitor were recorded. The pulse wave was defined as the value obtained by dividing the distance between the two points by the time spent in transferring the pulse. In the current study, the pulse wave was measured in the brachial artery and ankle (baPWV). The ABI was defined as the ratio between the systolic pressure measured in the ankle and that measured in the brachial artery.

Laboratory evaluation

In the morning, after an overnight fast, venous blood was sampled for the measurement of serum concentrations of glucose, total cholesterol, triglycerides and standard CRP.

Statistical analysis

Data are expressed as mean (S.D.). Differences between data were studied using the Student's *t* test. Analytical statistics of data between group comparisons of categorical data parameters were performed by using the chi-square test. Statistical significance was taken as $P < 0.05$. All statistical analyses were performed using JMP8 (SAS Institute, Tokyo, Japan).

Results

Clinical characteristics of the study group are presented in Table 1. Age, sex and triglyceride levels were similar between patients with CINCA syndrome and control subjects ($P = 0.65$, 0.53 and 0.17, respectively). Total cholesterol levels in CINCA syndrome patients were significantly lower than those in healthy controls, although they were within normal ranges in both groups. CRP concentrations in the patient group were significantly higher than in healthy controls [5.76 mm (S.D. 2.05) *vs* 0.08 (0.16), $P < 0.0001$].

All subjects tolerated the sonographic examination well. Sonographic study results and normal values of the parameters for the age of the patients [13, 14] are summarized in Table 2. Carotid artery analysis revealed that the IMT and stiffness parameter β of patients with CINCA syndrome were significantly higher than those of healthy controls [0.51 mm (S.D. 0.05) *vs* 0.44 (0.04), $P = 0.0021$, and 6.1 (S.D. 1.7) *vs* 3.9 (1.0), $P = 0.018$, respectively).

TABLE 1 Clinical and laboratory characteristics of the subjects

	Patient 1	Patient 2	Patient 3	CINCA syndrome ($n=3$), mean (S.D.)	Controls ($n=19$), mean (S.D.)	P-value
Gender, male/female	Male	Female	Male	2/1	9/10	0.53
Age, years	5	7	15	9.0 (5.3)	9.3 (4.3)	0.65
BMI, kg/m^2	16.0	15.5	16.8	16.1 (0.6)	17.3 (2.9)	0.51
Systolic blood pressure, mmHg	91	96	128	105 (20)	99 (8)	0.38
Diastolic blood pressure, mmHg	45	50	68	54 (12)	53 (4)	0.73
Total cholesterol, mg/dl	123	122	131	125 (5)	159 (17)	0.0046
Triglycerides, mg/dl	61	79	157	99 (51)	70 (28)	0.17
Glucose, mg/dl	93	85	102	94 (3)	94 (6)	0.95
CRP, mg/dl	0.26	1.62	5.55	2.48 (2.75)	0.08 (0.16)	<0.0001

CINCA syndrome: chronic infantile neurological cutaneous and articular syndrome.

TABLE 2 Ultrasonographic examination, baPWV and ABI in CINCA syndrome patients and control subjects

	Patient 1	Patient 2	Patient 3	CINCA syndrome ($n=3$), mean (S.D.)	Controls ($n=19$), mean (S.D.)	P-value
Intima–media thickness, mm (normal value for each age) [13]	0.47 (0.40)	0.5 (0.40)	0.57 (0.50)	0.51 (0.05)	0.44 (0.04)	0.0021
Systolic diameter, mm	5.5	5.8	5.8	5.7 (0.2)	6.2 (0.8)	0.30
Diastolic diameter, mm	4.8	5.2	5.4	5.1 (0.3)	5.3 (1.7)	0.63
Stiffness parameter β (normal value for each age) [14]	4.8 (3.4)	5.7 (3.7)	7.6 (4.5)	6.1 (1.7)	3.9 (1.0)	0.018
Right baPWV, cm/s	1068	920	1566	1185 (338)	850 (114)	0.0025
Left baPWV, cm/s	1053	1022	1587	1221 (318)	859 (114)	0.0014
Averaged baPWV, cm/s (normal value for each age) [15]	1061 (<941)	971 (<919)	1577 (1041)	1203 (328)	855 (114)	0.0017
Right ABI	1.15	0.91	0.98	1.00 (0.10)	1.04 (0.10)	0.67
Left ABI	1.16	0.95	0.92	0.99 (0.10)	1.06 (0.10)	0.48
Averaged ABI (normal value for each age) [15]	1.16 (>1.00)	0.93 (>1.00)	0.95 (>1.00)	0.99 (0.10)	1.05 (0.10)	0.54

CINCA syndrome: chronic infantile neurological cutaneous and articular syndrome; baPWV: brachial artery pulse wave velocity; ABI: ankle-brachial index.

The averaged baPWV of the patients was significantly higher than that of controls [1203 cm/s (S.D. 328) *vs* 855 (114), $P=0.017$) (Table 2). There was no significant difference in ABI between the two groups, although the values of two patients were lower than the normal range [15].

Discussion

In the present study we found that patients with CINCA syndrome develop atherosclerosis from early childhood. There have been many previous studies describing atherosclerosis associated with inflammatory diseases such as RA, SLE and FMF [1]. However, this is the first report showing the youngest group of patients who developed atherosclerosis associated with inflammatory disorders.

It has been shown that inflammation plays an important role in the development of atherosclerosis. The presence of macrophages and activated lymphocytes within the plaques supports the nature of an immune system-mediated inflammatory disorder of atherosclerosis. It has been shown that higher disease activity representing higher inflammatory burden is associated with increased cardiovascular events in patients with RA and SLE [16]. It may be induced by elevated inflammatory cytokines, which can cause the development of endothelial dysfunction in atherosclerotic processes. In addition, changes in lipid metabolism and a wide variety of immune and inflammatory alterations that directly affect the endothelium, vascular smooth muscle cells and inflammatory cellular components of the atherosclerotic plaque may also play important roles in the development and progression of atherosclerosis in patients. CINCA syndrome is the most severe form of CAPS, and patients display severe systemic inflammation from the neonatal period [3].

Therefore it is reasonable to assume that the progression of atherosclerosis from childhood in three patients with CINCA syndrome is closely related to chronic systemic inflammation. It was reported that the incidence of atherosclerosis could be reduced by aggressive disease-modifying therapies in patients with RA and SLE [16]. In patients with CINCA syndrome, we can investigate the association between inflammation and atherosclerosis without any effect of classical risk factors such as obesity, smoking, hyperlipidaemia or diabetes. This may provide a novel clue to clarify the role of inflammation in the development of atherosclerosis.

In patients with FMF and SLE, age and disease duration were reported to be associated with the severity of atherosclerosis [17]. In the present study we found that the oldest patient (patient 3) with the longest disease duration had the most advanced atherosclerosis, which is in line with this report. Early diagnosis and effective treatment for chronic inflammation in these patients have been emphasized in preventing cardiovascular disease because a negative correlation between the duration of anti-inflammatory treatment and IMT has been observed in SLE patients [18].

Interestingly, improvements in PWV and cIMT [19] were reported in patients with RA after sufficient infliximab treatment. In patients with CINCA syndrome, canakinumab was reported to induce rapid and sustained remission of symptoms [20]. It is possible that a significant improvement in atherosclerosis will be observed in our patients with CINCA syndrome after canakinumab treatment in the near future.

However, there are some limitations in the present study. First, our study contains only a small number of patients because of the extremely rare incidence of this disease. Second, the parameters investigated in this study are considerably variable with the age of the subjects. It is also possible that the values of the parameters change because of the measurement equipment. Multicentre and long-term follow-up analysis with standardized procedures and tools on a larger number of the patients are necessary to provide more precise information on the pathogenesis of atherosclerosis.

Conclusion

Patients with CINCA syndrome developed atherosclerosis from early childhood. Atherosclerosis in CINCA syndrome patients may be a prototype of cardiovascular disease predominantly induced by chronic inflammation.

Rheumatology key messages

- Patients with CINCA syndrome develop atherosclerosis from early childhood.
- This report shows the youngest group of patients who developed atherosclerosis associated with inflammatory disorders.
- Early treatment with anti-IL-1β antibody might be beneficial in preventing atherosclerosis in CINCA syndrome.

Acknowledgements

We thank Junji Kishimoto (Digital Medicine Initiative, Kyushu University Hospital, Fukuoka, Japan) for the contribution of statistical analysis.

Funding: This work was supported by a grant for Research on Intractable Diseases from the Ministry of Health, Labour and Welfare of Japan to T.H. and a grant-in-aid for scientific research from the Ministry of Education, Culture, Sports, Science, and Technology of Japan (24791072) to K.Y.

Disclosure statement: The authors have declared no conflicts of interest.

References

1 Tyrrell PN, Beyene J, Feldman BM *et al*. Rheumatic disease and carotid intima-media thickness: a systematic review and meta-analysis. Arterioscler Thromb Vasc Biol 2010;30:1014–26.

2 Kavey RE, Allada V, Daniels SR *et al*. Cardiovascular risk reduction in high-risk pediatric patients: a scientific statement from the American Heart Association Expert Panel on Population and Prevention Science; the Councils on Cardiovascular Disease in the Young, Epidemiology and Prevention, Nutrition, Physical Activity and Metabolism, High Blood Pressure Research, Cardiovascular Nursing, and the Kidney in Heart Disease; and the Interdisciplinary Working Group on Quality of Care and Outcomes Research: endorsed by the American Academy of Pediatrics. Circulation 2006;114:2710–38.

3 Kubota T, Koike R. Cryopyrin-associated periodic syndromes: background and therapeutics. Mod Rheumatol 2010;20:213–21.

4 Peters SA, den Ruijter HM, Bots ML, Moons KG. Improvements in risk stratification for the occurrence of cardiovascular disease by imaging subclinical atherosclerosis: a systematic review. Heart 2012;98:177–84.

5 Jarvisalo MJ, Putto-Laurila A, Jartti L *et al*. Carotid artery intima-media thickness in children with type 1 diabetes. Diabetes 2002;51:493–8.

6 Hirai T, Sasayama S, Kawasaki T, Yagi S. Stiffness of systemic arteries in patients with myocardial infarction. A noninvasive method to predict severity of coronary atherosclerosis. Circulation 1989;80:78–86.

7 Hirata K, Kawakami M, O'Rourke MF. Pulse wave analysis and pulse wave velocity: a review of blood pressure interpretation 100 years after Korotkov. Circ J 2006;70:1231–9.

8 Vlachopoulos C, Aznaouridis K, Terentes-Printzios D, Ioakeimidis N, Stefanadis C. Prediction of cardiovascular events and all-cause mortality with brachial-ankle elasticity index: a systematic review and meta-analysis. Hypertension 2012;60:556–62.

9 Takada H, Ishimura M, Inada H *et al*. Lipopolysaccharide-induced monocytic cell death for the diagnosis of mild neonatal-onset multisystem inflammatory disease. J Pediatr 2008;152:885–7.

10 Takada H, Kusuhara K, Nomura A *et al.* A novel CIAS1 mutation in a Japanese patient with chronic infantile neurological cutaneous and articular syndrome. Eur J Pediatr 2005;164:785–6.

11 Saito M, Nishikomori R, Kambe N *et al.* Disease-associated CIAS1 mutations induce monocyte death, revealing low-level mosaicism in mutation-negative cryopyrin-associated periodic syndrome patients. Blood 2008;111: 2132–41.

12 Mitsnefes MM, Kimball TR, Witt SA *et al.* Abnormal carotid artery structure and function in children and adolescents with successful renal transplantation. Circulation 2004; 110:97–101.

13 Jourdan C, Wuhl E, Litwin M *et al.* Normative values for intima-media thickness and distensibility of large arteries in healthy adolescents. J Hypertens 2005;23: 1707–15.

14 Sato A, Ichihashi K, Momoi M. Stiffness parameter B: changes with age in normal children. Neurosonology 2007;20:124–8.

15 Niboshi A, Hamaoka K, Sakata K, Inoue F. Characteristics of brachial-ankle pulse wave velocity in Japanese children. Eur J Pediatr 2006;165:625–9.

16 Roman MJ, Shanker BA, Davis A *et al.* Prevalence and correlates of accelerated atherosclerosis in systemic lupus erythematosus. N Engl J Med 2003;349: 2399–406.

17 Ugurlu S, Seyahi E, Cetinkaya F *et al.* Intima-media thickening in patients with familial Mediterranean fever. Rheumatology 2009;48:911–5.

18 Ristic GG, Lepic T, Glisic B *et al.* Rheumatoid arthritis is an independent risk factor for increased carotid intima-media thickness: impact of anti-inflammatory treatment. Rheumatology 2010;49:1076–81.

19 Del Porto F, Lagana B, Lai S *et al.* Response to anti-tumour necrosis factor alpha blockade is associated with reduction of carotid intima-media thickness in patients with active rheumatoid arthritis. Rheumatology 2007;46: 1111–5.

20 Kone-Paut I, Lachmann HJ, Kuemmerle-Deschner JB *et al.* Sustained remission of symptoms and improved health-related quality of life in patients with cryopyrin-associated periodic syndrome treated with canakinumab: results of a double-blind placebo-controlled randomized withdrawal study. Arthritis Res Ther 2011;13: R202.

THROMBOSIS AND HEMOSTASIS

Novel FV mutation (W1920R, FV_{Nara}) associated with serious deep vein thrombosis and more potent APC resistance relative to FV_{Leiden}

Keiji Nogami,[1] Keiko Shinozawa,[2] Kenichi Ogiwara,[1] Tomoko Matsumoto,[1] Kagehiro Amano,[2,3] Katsuyuki Fukutake,[2,3] and Midori Shima[1]

[1]Department of Pediatrics, Nara Medical University, Nara, Japan; [2]Department of Molecular Genetics of Coagulation Disorders and [3]Department of Laboratory Medicine, Tokyo Medical University, Tokyo, Japan

Key Points

- FV_{Nara} (W1920R), associated with serious deep vein thrombosis, is more resistant to APC relative to FV_{Leiden} (R506Q).
- This mechanism results from significant decreases in FVa susceptibility to APC and FV cofactor activity for APC.

Factor V (FV) appears to be pivotal in both procoagulant and anticoagulant mechanisms. A novel homozygote (FV_{Nara}), a novel mechanism of thrombosis associated with Trp1920→Arg (W1920R), was found in a Japanese boy and was associated with serious deep vein thrombosis despite a low level of plasma FV activity (10 IU/dL). Activated partial thromboplastin time–based clotting assays and thrombin generation assays showed that FV_{Nara} was resistant to activated protein C (APC). Reduced susceptibility of FVa_{Nara} to APC-catalyzed inactivation and impaired APC cofactor activity of FV_{Nara} on APC-catalyzed FVIIIa inactivation contributed to the APC resistance (APCR). Mixtures of FV-deficient plasma and recombinant FV-W1920R confirmed that the mutation governed the APCR of FV_{Nara}. APC-catalyzed inactivation of FVa-W1920R was significantly weakened, by ~11- and ~4.5-fold, compared with that of FV–wild-type (WT) and FV_{Leiden} (R506Q), respectively, through markedly delayed cleavage at Arg506 and little cleavage at Arg306, consistent with the significantly impaired APC-catalyzed inactivation. The rate of APC-catalyzed FVIIIa inactivation with FV-W1920R was similar to that without FV, suggesting a loss of APC cofactor activity. FV-W1920R bound to phospholipids, similar to FV-WT. In conclusion, relative to FV_{Leiden}, the more potent APCR of FV_{Nara} resulted from significant loss of FVa susceptibility to APC and APC cofactor activity, mediated by possible failure of interaction with APC and/or protein S. (*Blood.* 2014;123(15):2420-2428)

Introduction

Factor V (FV) contributes to opposing mechanisms in the regulation of coagulation.[1,2] The procoagulant action of FV is associated with cofactor activity for FXa in the prothrombinase complex, which catalyzes the conversion of prothrombin to thrombin on a phospholipid (PL) surface.[3-5] FV is converted to FVa by proteolytic cleavage by thrombin. Development of a hypercoagulant state is controlled by downregulation by activated protein C (APC) with protein S (PS). Hence, FVa is rapidly inactivated by proteolytic cleavage of the heavy chain (HCh) at Arg306, Arg506, and Arg679.[6,7] Cleavage at Arg506 is essential for the exposure of other cleavage sites but is not directly required for the decrease in activity. Cleavage at Arg306 results in near-complete loss of FVa activity. Nevertheless, any defect of 1 or more cleavage reactions significantly affects the processes of APC-induced inactivation.[8,9] The alternative function of FV is as an anticoagulant cofactor of APC in FVIIIa inactivation.[1] FVIIIa functions as a cofactor in the tenase complex and is responsible for PL-dependent FXa generation by FIXa.[10-12] In the process of APC-induced FVIIIa inactivation, FV acts as an anticoagulant cofactor of APC with PS, resulting in acceleration of FVIIIa inactivation through cleavage at Arg336.[13,14] This anticoagulant activity of FV is mediated by a product of proteolysis by APC before cleavage by thrombin. Cleavage at Arg506 of FV attached to the B domain is essential to the anticoagulant activity of FV, whereas cleavage at Arg306 appears to contribute less to this mechanism.[15,16] Any molecular defect of these cleavage reactions confers APC resistance (APCR).[1]

A point mutation of the *F5* gene, Arg506→Gln (R506Q; FV_{Leiden}), is the major cause of APCR[2] and is detected in ~20% of Caucasians with deep venous thrombosis (DVT).[17,18] The loss of the APC cleavage site at Arg506 in FV_{Leiden} results in a loss of APC-induced FVa inactivation and impairment of FV cofactor activity of APC in FVIIIa inactivation. Rare FV point mutations Arg306→Thr (R306T; $FV_{Cambridge}$)[19,20] and Arg306→Gly (R306G; $FV_{Hong\ Kong}$)[20,21] affect the APC cleavage site at Arg306 and are associated with mild APCR.[22] No FV mutations linked to APCR have been identified in Japanese populations, however. We describe the findings in a Japanese boy with severe DVT in the paradoxical presence of FV deficiency with FV activity (FV:C) 10 IU/dL. We have identified a novel mechanism of thrombosis associated with a Trp1920→Arg (W1920R) mutation in the *F5* gene (FV_{Nara}). The defect resulted in APCR more potent than that seen with FV_{Leiden}.

Submitted October 1, 2013; accepted January 28, 2014. Prepublished online as *Blood* First Edition paper, February 12, 2014; DOI 10.1182/blood-2013-10-530089.

K.N. and K.S. contributed equally to this study.

Presented in abstract form at the 53rd annual meeting of the American Society of Hematology, San Diego, CA, December 12, 2011.

There is an Inside *Blood* Commentary on this article in this issue.

The publication costs of this article were defrayed in part by page charge payment. Therefore, and solely to indicate this fact, this article is hereby marked "advertisement" in accordance with 18 USC section 1734.

© 2014 by The American Society of Hematology

Materials and methods

Blood samples were obtained after informed consent following local ethical guidelines. DNA direct sequencing and the expression of recombinant protein were approved by the Medical Research Ethics Committee of Tokyo Medical University. This study was conducted in accordance with the Declaration of Helsinki.

Reagents

The pMT2/FV mammalian expression plasmid containing the full-length *F5* cDNA was provided by Dr Kaufman (University of Michigan, Ann Arbor, MI). The EZ1 DNA Blood Kit, QIAquick Gel Extraction Kit, and QIAfilter Plasmid Kit (Qiagen, Dusseldorf, Germany) and the QuickChange Site-Directed Mutagenesis Kit (Stratagene, La Jolla, CA) were purchased. Recombinant FVIII was a generous gift from Bayer Corporation, Japan. A monoclonal antibody (mAb)C5,[23] recognizing the C-terminus of the FVIII A1 domain, was provided by Dr Carol Fulcher (Scripps Research Institute, La Jolla, CA). FV, FIXa, FX, FXa, α-thrombin, APC, PS, mAbAHV-5146 against the FV HCh (Hematologic Technologies, Essex Junction, VT), lipidated TF (Innovin; Dade Behring, Marburg, Germany), and fluorogenic substrate Z-Gly-Gly-Arg-AMC (Bachem, Bubendorf, Switzerland) were purchased commercially. FV-deficient plasmas (George King. Overland Park, KS), PT, and activated partial thromboplastin time (aPTT) reagent (Instrumentation Laboratory, Bedford, MA; Sysmex, Kobe, Japan) were purchased. PL vesicles containing phosphatidylserine/phosphatidylcholine/phosphatidylethanolamine, 10%/60%/30%, were prepared using *N*-octylglucoside.[24]

DNA direct sequencing

Genomic DNA was extracted from leukocytes, using the BioRobot EZ1 workstation. PCR assays were performed with *Taq* DNA polymerase (TaKaRa-Bio, Otsu, Japan). PCR products were electrophoresed on agarose gels and purified by gel extraction. Purified PCR products from genomic DNA and *F5* plasmids were confirmed by sequencing using a BigDye Terminator v3.1 Cycle Sequencing kit (Applied Biosystems) and analyzed with a 3730 DNA analyzer. All sequences were compared with wild-type (WT) *F5* sequences (GenBank number Z99572).

Expression of recombinant FV

The mutations were introduced independently into a pMT2/FV plasmid by site-directed mutagenesis.[25] The WT and mutant plasmids used in transfection experiments were purified. Vectors expressing recombinant proteins were transfected into HEK293 cells, using the lipofection method. After 60 hours, the culture media and cells were harvested. Conditioned media (CM) were collected, centrifuged to remove cell debris, and stored at −80°C. FV antigen (FV:Ag) levels in CM and cell lysates were measured by enzyme-linked immunosorbent assay (ELISA; Affinity Biologicals). FV:C in CM was measured in PT-based clotting assays, using the ACL9000 coagulation analyzer (Instrumentation Laboratory). The specific activity of FV was calculated as the ratio of FV:C to the concentration of FV:Ag, both of which were measured in CM. The proteins were harvested in serum-free medium and concentrated by filtration (cutoff ~100 kDa).

APCR assay

aPTT-based assays. The APC-resistance kit, which is not approved and not commercially available in Japan, was provided by Instrumentation Laboratory for research use. This assay was performed using ACL9000 with predilution of sample plasmas in FV-deficient plasma. The APC sensitivity ratios (APCsrs) were expressed as ratios of aPTT clotting times in the presence of APC divided by clotting times in its absence. This assay reflects the effect of APC on inactivation of both FVa and FVIIIa; hence, a low level of APCsr indicates a defect in the inactivation of FVa and/or FVIIIa and, consequently, reflects APCR.

Thrombin generation-based assays. Calibrated automated thrombin generation assay (Thrombinoscope) was performed as previously reported.[26] Platelet-poor plasma (PPP) or platelet-rich plasma (PRP) was preincubated for 10 minutes with TF (5 pM), APC (8 or 40 nM), and PL (0 or 10 μM), respectively. PRP was adjusted to 15×10^4 platelets/μL. Measurements were commenced after the addition of $CaCl_2$ and fluorogenic substrate (final concentration [f.c.] 16.7 mM and 417 μM, respectively). Fluorescent signals were monitored continuously in a Fluoroskan microplate reader (Thermo Fisher Scientific, Franklin, MA). For data analyses, the parameters (lag time, peak thrombin, time to peak, and endogenous thrombin potential [ETP]) were derived. The APCsrs were expressed as ratios of the parameter in the absence (or presence) of APC, divided by the ratio in its presence (or absence).

FXa generation-based assays. Normal or patient's plasma was mixed with FV-deficient plasma in various proportions and assayed using the FXa generation assay (COATEST SP-FVIII, Chromogenix, Milan, Italy), with minor modifications.[27] The test specifically quantifies FVIIIa:C in 16-fold diluted plasma by measuring intrinsic FXa generation mediated by excess exogenous FIXa and FX with PL. The simultaneous addition of APC (40 nM) with cofactors PS and FV in plasma inhibits intrinsic FXa generation by inactivating FVIIIa. The APCsrs were expressed as ratios of the amount of generated FXa in the absence of APC divided by that in its presence. A low level of APCsr indicates a defect in FVIIIa inactivation and, consequently, reflects APCR.

Prothrombinase assay

FV (2 nM) was activated by thrombin (20 nM) for 1 minute, followed by the addition of hirudin. The reactants were mixed with prothrombin (1.4 μM), PL, and 5-dimethylamino-naphthalene-1-sulfonylarginine-*N*-(3-ethyl-1,5-pentanediyl)-amide (30 μM), followed by initiation by the addition of FXa (10 pM). Aliquots were removed to assess the initial rates of product formation, and the reactions were quenched with EDTA (f.c. 50 mM). Rates of thrombin generation were determined at absorbance 405 nm (Abs_{405}) after the addition of S-2238 (f.c. 0.46 mM). Thrombin generation was quantified from a standard curve prepared using known amounts of thrombin.

FV–PL binding

Binding of FV to immobilized PL was examined in ELISAs.[28] α-phosphatidyl-*L*-serine (5 μg/mL) in methanol was added to microtiter wells and air-dried. The wells were blocked by the addition of gelatin solution (5 mg/mL), and serial dilutions of FV were added and incubated at 37°C for 2 hours. Bound FV was quantified by the addition of anti-FV mAbAHV-5146 (2.5 μg/mL) and goat anti-mouse peroxidase-linked antibody, followed by measuring at Abs_{492}. The amount of nonspecific immunoglobulin G (IgG) binding without FV was <3% of the total signal. Specific binding was estimated by subtracting the amount of nonspecific binding.

APC-catalyzed inactivation of FVa

FV (8 nM) was incubated with thrombin (100 nM) for 5 minutes at 37°C, and reaction was terminated by the addition of hirudin (25 U/mL). Samples containing the generated FVa (2 nM) were incubated with APC (25 pM), and PS (30 nM) with PL (20 μM), for the indicated times. Aliquots were obtained from the mixtures and diluted ~30-fold. Residual FV:C was measured in aPTT-based clotting assays. The presence of thrombin and hirudin in the diluted samples had little effect in these assays.

APC cofactor activity of FV

The APC cofactor activity of FV variants was measured in a FVIIIa degradation assay,[29] with minor modifications. FVIII (10 nM) and PL (20 μM) were activated by thrombin (5 nM) for 30 seconds, and the reaction was terminated by the addition of hirudin (2.5 U/mL). The generated FVIIIa was then incubated with APC (0.5 nM) and PS (5 nM) with various concentrations of FV variants for 20 minutes. The reactants were diluted 9-fold before incubation with FIXa (2 nM) and FX (200 nM) for 1 minute. Generated FXa was measured in a chromogenic assay with S-2222 at Abs_{405}. Relative FVIII:C was calculated from the amounts of generated FXa.

Table 1. FV levels and APCR in plasmas of the patient and family members

Case	FV:C (IU/dL)	FV:Ag (IU/dL)	*F5* mutation	aPTT-based APCR assay		
				aPTT, seconds		
				Minus APC	Plus APC	APCsr (plus/minus APC)
FV_{Nara} family members						
Patient	10.0	40.0	W1920R homozygote	79.7	131	1.64
Father	74.1	74.0	W1920R heterozygote	43.3	98.0	2.26
Mother	87.6	75.0	W1920R heterozygote	39.0	104	2.67
Brother	109	77.0	WT	32.2	98.4	3.06
Sister-1	113	101	WT	32.6	107	3.28
Sister-2	132	115	WT	32.2	99.8	3.10
FV_{Leiden} patient						
Patient 1	56.5	96.0	R506Q heterozygote	35.2	57.2	1.63
Patient 2	65.2	61.0	R506Q heterozygote	36.8	61.2	1.66
FV-deficient patient						
Patient 1	50.0	44.0		39.2	124	3.16
Patient 2	54.0	53.0		38.4	118	3.07
Patient 3	55.0	47.0		43.4	124	2.85
Healthy controls						
Male (n = 17)				32.6 ± 0.70	108.4 ± 4.50	3.32 ± 0.11
Female (n = 15)				33.5 ± 1.47	108.6 ± 3.64	3.24 ± 0.08

All data were measured at least 3 times, and the average values are shown. For the levels of healthy controls, the average value ± standard deviation is shown.

Western blotting

Sodium dodecyl sulfate/polyacrylamide gel electrophoresis was performed using 8% gels, followed by western blotting.[30] Protein bands were probed using the indicated mAbs, followed by the addition of goat anti-mouse peroxidase-linked antibody.[30] Signals were detected using enhanced chemiluminescence, and densitometric scans were quantified using Image J 1.34.

Results

Patient's profile

A 13-year-old boy was admitted for massive DVT in association with swelling of the lower extremities. There was no personal or family history of thrombosis. Laboratory findings demonstrated prolonged PT and aPTT (18.9/67.6 seconds; control, 12.2/30.2 seconds). FV:C and FV:Ag were 10 and 40 IU/dL, respectively, indicating a cross-reactive material–reduced reaction. Anti-FV inhibitor was not detected. Other procoagulant and anticoagulant factors, including fibrinolytic factors and antiphospholipid syndrome-associated factors, were within normal range. Free tissue factor pathway inhibitor was 20.2 ng/mL (normal, 15-35 ng/mL).[31] His parents and 3 siblings had normal levels of FV:C and FV:Ag (Table 1). He was treated with warfarin to maintain prothrombin time-international normalized ratio 2.5 to 3.0. Nevertheless, a fresh thrombus developed in his left external iliac-vein, and the right inferior vena cava was completely occluded. After heparinization and urokinase therapy, the patient was treated with higher doses of warfarin to maintain prothrombin time-international normalized ratio 4.0 to 5.0, and he has since been free of recurrent DVT.

Gene analysis

Direct sequencing identified a W1920R homozygous mutation of exon 20 of *F5* in the patient (Figure 1). His parents heterozygously carried this mutation, but it was undetected in his siblings. Neither the FV_{Leiden} mutation (R506Q) nor FV-HR2 haplotype (H1299R and D2194G) were found in the patient or his family members. The W1920R mutation was not detected in 100 alleles from Japanese control subjects using direct sequencing, and the novel *F5* missense mutation that we identified was designated FV_{Nara}.

APCR in FV_{Nara} plasma

We investigated whether the FV_{Nara} was resistant to APC. aPTT-based APCR assays, reflecting APC inactivation of FVa and FVIIIa, were performed. The APCsr obtained in patient's plasma was similar to those of FV_{Leiden} patients and significantly lower than those in healthy control patients (Table 1). APCsrs in the parents were intermediate, and those in the siblings were equal to the levels of healthy controls. APCsrs of 3 mild FV-deficient patients with FV:C ~50 IU/dL were similar to those of control. APCsrs of inherited FV-deficient patients with FV:C ~10 IU/dL were not measurable, however, because the clotting times after the addition of APC were markedly prolonged (data not shown). These results demonstrated that the FV_{Nara} mutation conferred APCR.

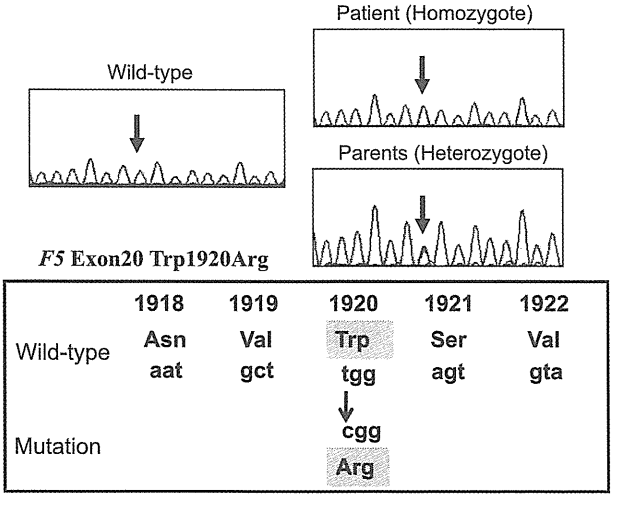

Figure 1. DNA direct sequencing of exon 20 of *F5* gene from the patient, his parents, normal WT. The mutation (T–C) is present at codon 1920, resulting in a Trp1920→Arg substitution in the FV protein (FV_{Nara}).

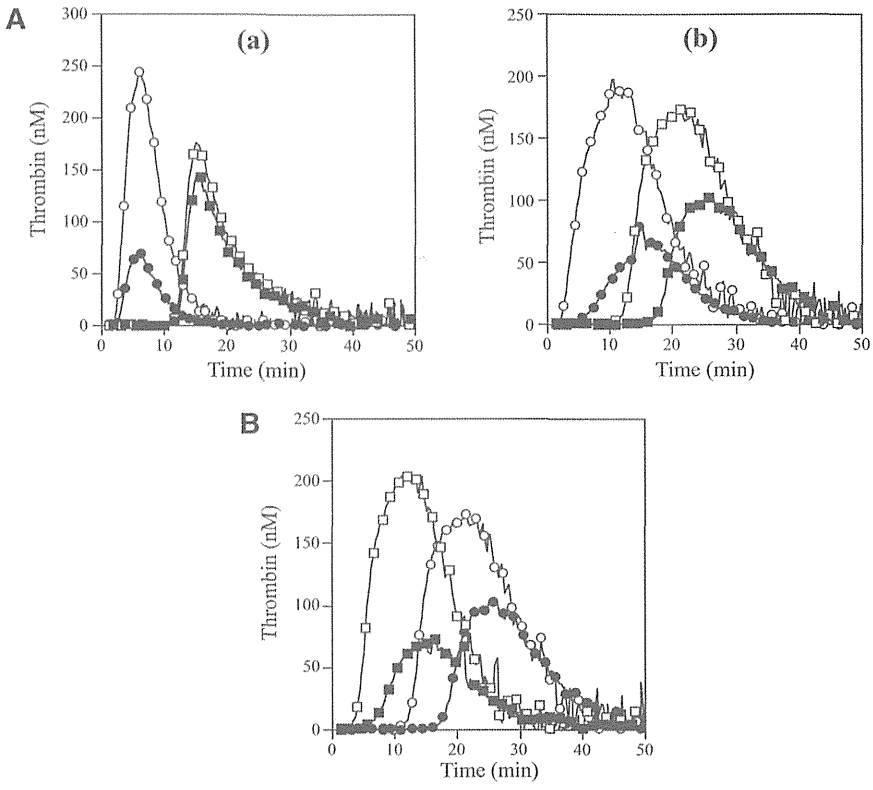

Figure 2. Thrombin generation in the FV_{Nara} patient's plasma. (A) Effects of the addition of APC: thrombin generation after extrinsic activation (TF; 5 pM) of PPP (a) or PRP (b) in normal individuals (circle symbols) and PPP (a) or PRP (b) in FV_{Nara} patient (square symbols) in the absence (open symbols) or presence (closed symbols) of APC was measured as described in "Materials and methods." With PPP, APC (8 nM) was added with PL vesicles (10 μM), whereas with PRP, APC (40 nM) was added without PL. A representative thrombogram is shown. (B) Effects of the addition of native FV: thrombin generation was measured after extrinsic activation (TF; 5 pM) of the patient's PRP with the addition of native FV (circles, 0 IU/dL; squares, 10 IU/dL) in the absence (open symbols) or presence (closed symbols) of APC (40 nM). All experiments were performed at least 3 separate times, and a representative thrombogram is shown.

APCR in the FV_{Nara} patient was examined using PPP in thrombin generation assay initiated by low concentrations of TF with APC. The time-related parameters (lag time and time to peak) and peak thrombin obtained with FV_{Nara} PPP were prolonged and decreased, respectively, compared with control (Figure 2Aa and Table 2). The addition of APC showed that the peak thrombin and ETP with FV_{Nara} were less moderated than those with control, although the time-related readings were unaffected. The APCsrs (minus APC/plus APC) with FV_{Nara} (1.22 and 1.25) were significantly lower than those with control (3.48 and 3.70), supportive of the APCR with FV_{Nara}. Platelet FV also participates in the clotting function of FV; to evaluate the role of platelet FV in these mechanisms, therefore, experiments were repeated using PRP. Similar to PPP, the addition of APC showed that APCsrs (plus APC/minus APC) in time-related parameters in FV_{Nara} were lower than those in control, and the APCsrs (minus APC/plus APC) with FV_{Nara} were also lower than those with control (Figure 2Ab). These findings provided further evidence of APCR with FV_{Nara}. Similar experiments in PPP using 40 nM APC (equal amount in PRP) showed that the thrombin generation of FV_{Nara}, as well as normal plasma, was little detected (data not shown), again confirming that the platelet FV was particularly resistant to APC-mediated inactivation.

To further assess the contribution of plasma FV in the APCR of FV_{Nara}, normal FV was added to the patient's PRP before measuring thrombin generation with APC (Figure 2B). In the presence of normal FV (10 IU/dL) corresponding to the level in patient's plasma, the time-related parameters were moderately shortened, and the peak thrombin and ETP were slightly increased. Thus, the presence of native FV improved reactivity to APC in FV_{Nara} PRP, suggesting that the APCR of FV_{Nara} might be caused by defective patient's plasma FV. Furthermore, even small amounts of plasma FV appeared to influence APC-induced deceleration of blood coagulation.

APC cofactor activity of FV_{Nara}

APCR resulting from a *F5* mutation or mutations is caused by a reduced sensitivity of FVa to APC-catalyzed inactivation[7,32] and/or reduced FV cofactor activity in APC-catalyzed FVIIIa inactivation,[33] but these components are difficult to distinguish. FXa generation

Table 2. Parameters obtained from thrombin generation on the PPP and PRP with FV_{Nara}

	Lag time (APC minus/plus, minutes [APCsr])*	Time to peak (APC minus/plus, minutes [APCsr])*	Peak thrombin (APC minus/plus, nM [APCsr])†	ETP (APC minus/plus, nM × minutes [APCsr])†
PPP				
Control	2.50/2.62 (1.05)	6.12/5.62 (0.92)	242/70 (3.48)	1648/446 (3.70)
FV_{Nara}	12.3/12.5 (1.02)	15.3/15.3 (1.00)	176/144 (1.22)	1711/1373 (1.25)
PRP				
Control	3.01/6.55 (2.18)	11.5/15.7 (1.36)	191/71 (2.69)	2860/968 (2.95)
FV_{Nara}	12.8/18.2 (1.42)	21.2/26.2 (1.23)	169/103 (1.64)	2811/1620 (1.74)
+ FV (10 IU/dL)	2.86/6.45 (2.25)	11.5/16.2 (1.42)	201/70 (2.87)	2988/930 (3.21)

Values were calculated from the parameter data obtained in Figure 2.
*Values were expressed as plus APC divided by minus APC.
†Values were expressed as minus APC divided by plus APC.

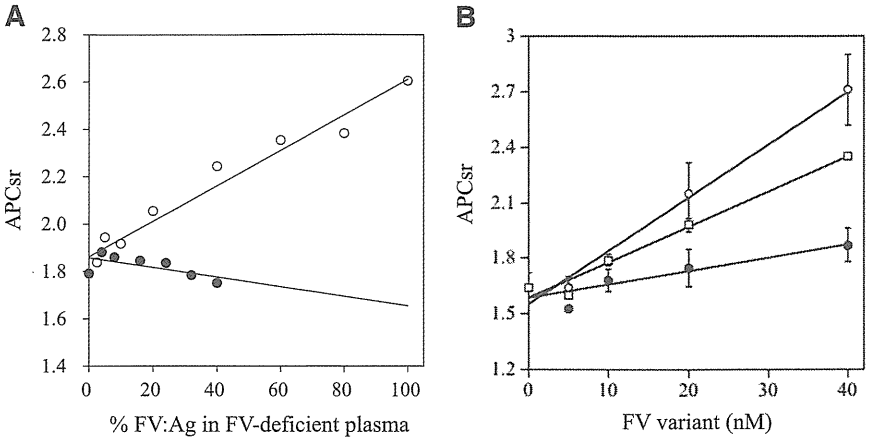

Figure 3. APCR in FXa generation assays. (A) Effects of FV levels on the APCsr in the FV_{Nara} plasma. Normal plasma (open circles) and the patient's plasma (closed circles) were mixed with FV-deficient plasma in various proportions, and FXa generation was measured with COATEST SP FVIII after the simultaneous addition of APC (40 nM) as described in "Materials and methods." The APCsrs were expressed as ratios of the amount of generated FXa in the absence of APC divided by that in its presence. All experiments were performed at least 3 separate times, and the average values are shown. (B) APCR of FV-deficient plasma mixed with recombinant FV-W1920R. Various concentrations of FV (WT, open circles; W1920R, closed circles; R506Q, open squares) were mixed with diluted FV-deficient plasma, and FXa generation was measured with COATEST SP FVIII after the simultaneous addition of APC (40 nM), as described in "Materials and methods." The APCsrs were expressed as ratios of the amount of generated FXa in the absence of APC divided by that in its presence. All experiments were performed at least 3 separate times, and the average and/or standard deviation values are shown.

assays, reflecting intrinsic tenase activity, were used to examine the APC cofactor activity of FV.[27] We therefore determined APCsrs in samples after the addition of APC to probe APCR resulting from defective FV cofactor activity. Normal or FV_{Nara} plasma was mixed with FV-deficient plasma in proportions from 2.5% to 100%. Because FV_{Nara}:Ag was 40 IU/dL, the concentration of FV_{Nara} in these assays varied between 2.5% and 40%. APCsrs increased linearly in proportion to the level of normal FV, and clear differences were demonstrated between 0% and 100% normal plasma (1.8 and 2.6, respectively), similar to an earlier report.[27] APCsrs were independent of the concentration of FV_{Nara}, however, and remained relatively constant or modestly decreased (Figure 3A). The slopes obtained with normal and FV_{Nara} plasmas (ΔAPCsr; 0.72 and −0.18/IU FV, respectively) were significantly different ($P < .01$), indicating that FV_{Nara} possessed little APC cofactor activity.

APCR of FV-W1920R mutant

The measurements of APCR of FV_{Nara} could have been affected by quantitative or qualitative abnormalities of individual plasma components other than FV. To confirm FV specificity, recombinant FV-WT and 2 FV mutant proteins (W1920R and R506Q) were prepared. The levels of FV:Ag and specific activity of the W1920R mutant expressed in CM were similar to the data observed with patient's plasma, at 50% and 45% of WT, respectively. Corresponding levels in CM of R506Q were 125% and 86% of WT, respectively.

APCR assays were repeated using mixtures of FV-deficient plasmas and recombinant FV variants. FXa generation assays were devised in which FV-deficient plasma and FV were diluted 16-fold before mixing with APC; this facilitated measurements at lower levels of FV:Ag (0.3-2.5 nM). These concentrations were comparable to diluted plasma containing physiological levels of FV:Ag (5-40 nM;

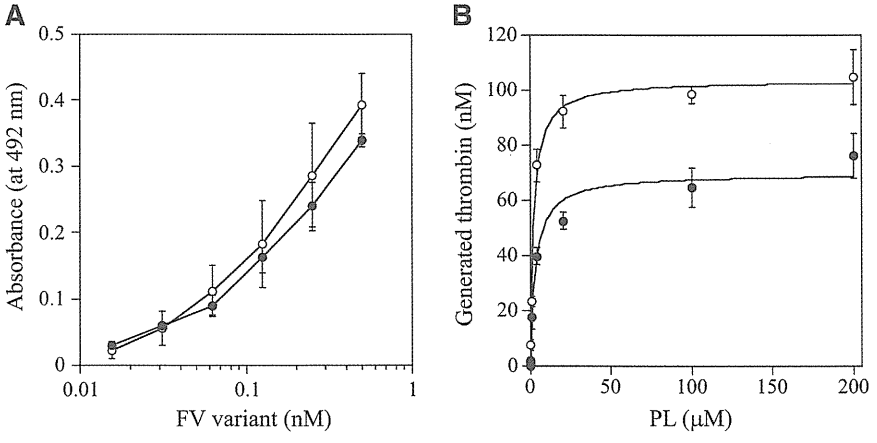

Figure 4. FV-W1920R affecting the association with PL. (A) FV-PL binding. α-Phosphatidyl-L-serine (5 μg/mL) was added to microtiter wells and air-dried. After blocking, serial dilutions of FV were added to the immobilized PL. Bound FV-WT (open circles) and FV-W1920R (closed circles) was quantified by the addition of AHV-5146, as described in "Materials and methods." The average values and standard deviations are shown. (B) The effects of PL on prothrombinase activity; FV (WT, open circles; W1920R, closed circles; 2 nM) was activated by thrombin (20 nM) for 1 minute, followed by the addition of hirudin. The reactants were incubated with prothrombin (1.4 μM) and various amounts of PL, followed by initiation by the addition of FXa (10 pM). Aliquots were removed, and the reactions were quenched by the addition of EDTA. Rates of thrombin generation were determined at Abs_{405} after the addition of S-2238. Thrombin generation was quantified by extrapolation from a standard curve prepared using known amounts of thrombin. The plotted data were fitted using the Michaelis-Menten equation. All experiments were performed at least 3 separate times, and the average values are shown.

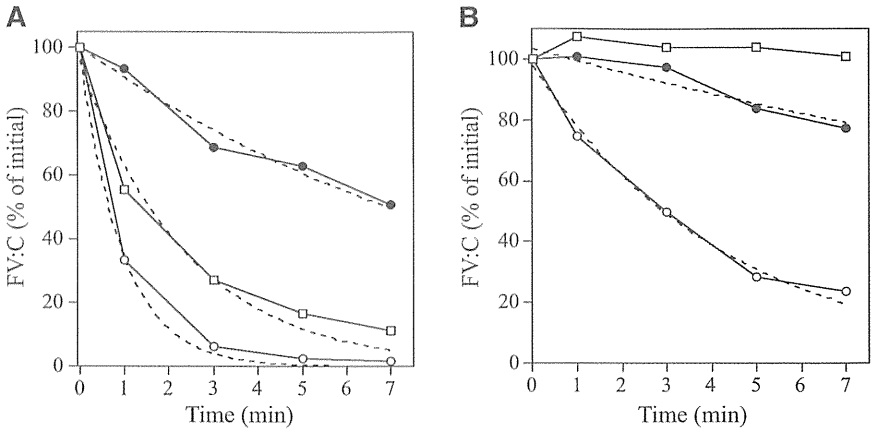

Figure 5. APC-mediated inactivation of FVa-W1920R mutant. FV variants (8 nM) were incubated with thrombin (100 nM) for 5 minutes, and the reaction was terminated by the addition of hirudin (25 U/mL). FVa variant samples (2 nM) were reacted with APC (25 pM) and PL (20 μM) in the presence (A) or absence (B) of PS (30 nM). After dilution, FVa activity was measured in an aPTT-based 1-stage clotting assay. The symbols used are as follows: open circles, WT; closed circles, W1920R; open squares, R506Q. Initial activities of FVa variants were regarded as 100%. The plotted data were fitted in an equation of single exponential decay. All experiments were performed at least 3 separate times, and the average values are shown.

15%-120% of normal FV:Ag). In mixtures with WT, APCsrs increased dose-dependently (ΔAPCsr; 2.85 × 10^{-2}/nM FV; Figure 3B). The APCsr in W1920R was lower by ~4-fold (0.71 × 10^{-2}/nM FV) than WT, in keeping with the impairment of APC cofactor activity in W1920R. With R506Q, the APCsr was greater by ~2.7-fold (1.91 × 10^{-2}/nM FV) than that with W1920R. These findings demonstrated that APCR in FV_{Nara} plasma resulted from W1920R, and the APC cofactor activity of W1920R appeared to be more defective than that of R506Q.

The C1 and/or C2 domains of FV(a) bind to PL membranes,[34,35] which governs the susceptibility of FVa for APC-catalyzed inactivation and the APC cofactor activity of FV. W1920 is in proximity to the PL-binding region or regions,[36] and we speculated that the APCR of FV-W1920R might be a result of significant disturbances in PL binding. The PL binding of W1920R was maintained at ~90% that of WT in ELISA, however (Figure 4A). The influence of PL on prothrombinase activity with W1920R was also investigated. Thrombin generation with W1920R was ~70% the level of that with WT, again supporting the cross-reactive material–reduced type on FV_{Nara}. However, the affinity of PL for W1920R was not significantly different compared with WT (K_m: 3.25 ± 0.77/2.22 ± 0.24 μM, respectively; Figure 4B). Thrombin and PL-dependent FXa activation of W1920R showed a similar reaction to the activation of WT (data not shown). These findings indicated that W1920R–PL interactions were not disturbed.

APC-catalyzed inactivation of FVa-W1920R

APC-catalyzed inactivation of FVa-W1920R, compared with the inactivation of WT and R506Q (FV_{Leiden}), were examined in 1-stage clotting assays. FVa-WT:C was very rapidly decreased after the addition of APC and PS and declined to ~2% of the initial level at 5 minutes (Figure 5A). FVa-R506Q:C was reduced to ~20% of the initial level at 5 minutes. Surprisingly, FVa-W1920R:C decreased very slowly and persisted at ~60% of the initial level. The inactivation rate of W1920R was ~11- and ~4.5-fold lower than the rates of WT and R506Q, respectively (Table 3), indicating significantly defective APC-induced inactivation of W1920R. Without PS, the inactivation rate of FVa-WT:C was significantly decreased, with ~20% of the rate obtained with PS (Figure 5B), whereas inactivation of FVa-R506Q:C was not observed. The inactivation rate of FVa-W1920R:C appeared to be ~40% less than that with PS, but this was ~6-fold lower than that of WT, supporting the theory that W1920R as a cofactor for PS contributed less to the mechanisms of APCR than WT and R506Q.

Sodium dodecyl sulfate/polyacrylamide gel electrophoresis of APC cleavage was designed to investigate the mechanism or mechanisms contributing to the defective APC-catalyzed inactivation of FVa-W1920R (Figure 6). Using FVa-WT, the band of residues 1 to 506 rapidly appeared within 20 seconds after the addition of APC, followed sequentially by the appearances of the 307 to 506 and 307 to 709 bands, consistent with rapid, consecutive cleavage at Arg506 and Arg306. Cleavage of FVa-R506Q at Gln506 was not evident during a 5-minute reaction. The appearance of the 307 to 709 band was evident at similar velocity to that in WT, but the total ratio of Arg306 cleavage in R506Q was reduced. The appearance of the 1 to 506 band in W1920R was markedly delayed compared with WT, however, and cleavage at Arg306 was not detected. These results suggested that the loss of APC-catalyzed inactivation of FVa-W1920R was a result of a significant delay in cleavage at Arg506 and little cleavage at Arg306.

Cofactor FV-W1920R on APC-catalyzed FVIIIa inactivation

Properties of FV-W1920R as a cofactor for APC were examined in a FVIIIa degradation assay.[29] FV-WT significantly enhanced APC-catalyzed FVIIIa inactivation with a ~3-fold inactivation rate compared with that in its absence, again confirming the APC cofactor activity of FV (Figure 7Aa and Table 4). FV-R506Q moderately diminished APC-catalyzed inactivation with the ~50% inactivation rate of WT. However, the rate with W1920R was similar to that in its absence, emphasizing earlier findings that APC cofactor activity was markedly depleted with W1920R. With regard to the effects of varying amounts of FV on APC cofactor activity, FV-WT enhanced the APC-catalyzed inactivation dose-dependently (50% reduction, 0.25 nM) (Figure 7Ab). Inactivation with R506Q was also enhanced, but the 50% reduction of 0.55 nM was greater than that with WT. However, even at 1 nM of W1920R, little enhancement of this mechanism was demonstrated, indicating that impairment of APC cofactor activity with W1920R was more pronounced than with R506Q.

Table 3. Kinetic parameters determined on APC-catalyzed inactivation of recombinant FVa variants

	PS, $minutes^{-1}$ (-fold)	
FVa variants	Plus	Minus
WT	1.07 ± 0.06 (1)	0.230 ± 0.016 (1)
W1920R	0.100 ± 0.001 (0.09)	0.038 ± 0.008 (0.16)
R506Q	0.417 ± 0.061 (0.39)	Not determined

Values were calculated by nonlinear least squares regression from the data shown in Figure 5A-B, using the single exponential decay.

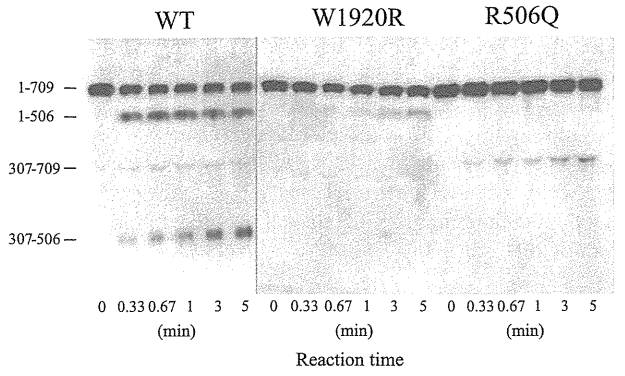

Figure 6. APC-catalyzed proteolytic cleavage of the HCh of FVa-W1920R. FV variants (8 nM) were incubated with thrombin (100 nM) for 5 minutes, and the reaction was terminated by the addition of hirudin (25 U/mL). FVa variant samples (0.5 nM) were incubated with APC (1 nM) and PS (30 nM) in the presence of PL (20 μM) for the indicated times. Samples were analyzed on 8% gels, followed by western blotting using an anti-FV HCh mAb 5146 IgG, as described in "Materials and methods." A vertical line is inserted to indicate a repositioned gel lane.

APC-catalyzed FVIIIa inactivation is regulated by cleavage at Arg336 in A1.[37] Figure 7B illustrates time-dependent cleavage at Arg336 analyzed by western blotting using mAbC5. This mAb recognizes the residues 337 to 372, and the disappearance of this band represents cleavage at Arg336.[38] With FV-WT, intact A1 gradually decreased time-dependently (Figure 7Ba). With FV-W1920R, however, cleavage at Arg336 was not observed during a 10-minute reaction time, and the rate of cleavage with FV-R506Q appeared to be ~40% of that of FV-WT (Figure 7Bb and Table 4), consistent with the results obtained in FXa generation assays. These data confirmed that APC cofactor activity was partially or completely impaired with R506Q and W1920R, respectively.

Discussion

We described a novel FV-W1920R missense mutation associated with APCR in a Japanese boy with serious DVT. The APCR of FV_{Nara} was greater than that of FV_{Leiden} and involved a novel mechanism related to a significant inhibition of cleavage at both sites because of the possible failure of direct and/or indirect interactions with APC and/or PS.

FV-W1920 is a highly conserved residue among other mammalians. According to the crystal structure of APC-inactivated bovine FVa,[36] bovine-W1907 (corresponding to human-W1920) is located on the internal structure in the C1 domain, which is involved in 3 spike-like structures of β-strand as PL-binding sites. W1907 forms hydrogen bonding with W1891 (W1904) and L2013 (L2026), which is located at the first and second spike of PL-binding, respectively. W1920R may have an effect on the PL binding at the C1 interface and may be an unstable molecule by modification (eg, misfolding). However, because a functional assay such as prothrombinase activity, FXa activation, and a PL-binding assay did not indicate significant differences between WT and W1920R, this molecule would be not significantly disturbed structurally; thereby, the reason for secretion defect is unclear.

Our assays for APC-catalyzed FV cleavage demonstrated little cleavage of W1920R at Arg306, and cleavage at Arg506 was markedly delayed. As discussed earlier, the Arg506 cleavage is considered to be essential for direct and FVIII-related anticoagulant properties of FV,[15,16,29] whereas the Arg306 cleavage is associated with FVa inactivation. Mutations at Arg306, including $FV_{Cambridge}$, contribute to mild APCR, and a similar mutation $FV_{Hong\ Kong}$, appears not to affect the APC response.[19-21] We speculate, therefore, that the impairment of APC-catalyzed cleavage at Arg506 in FV_{Nara} resulted in persistent levels of FVIIIa:C and FVa:C and was the

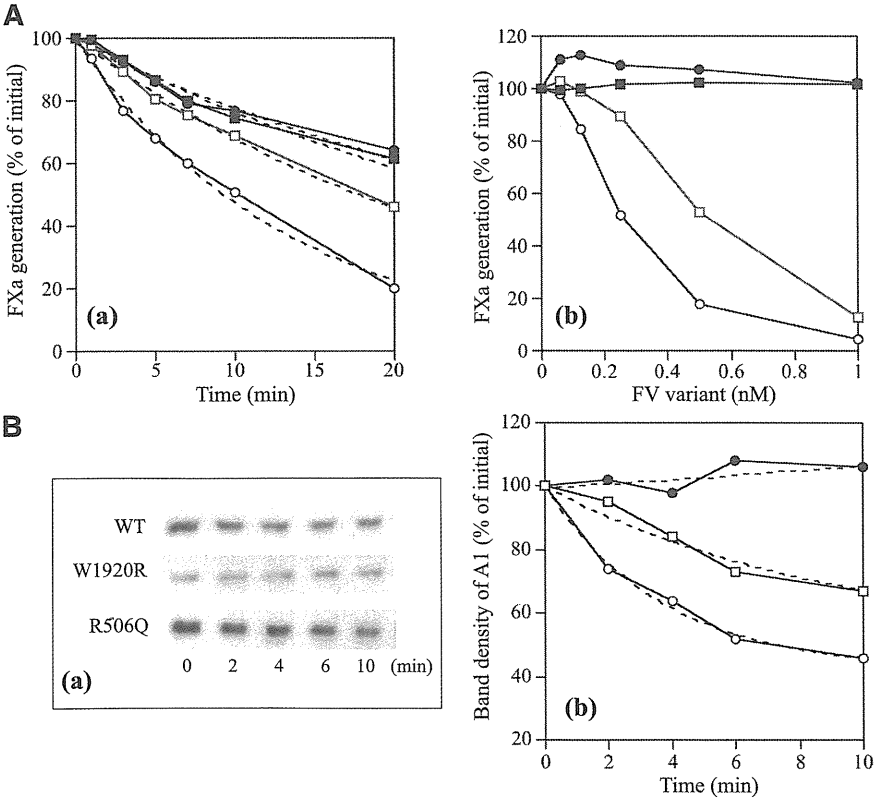

Figure 7. APC cofactor activity of FV-W1920R assessed by the degradation of FVIIIa. (A) FVIIIa inactivation. FVIII (10 nM) with PL (20 μM) was activated by thrombin (5 nM), followed by the addition of hirudin (2.5 U/mL). Generated FVIIIa was incubated either with mixtures of APC (0.5 nM), PS (5 nM), and FV variants (0.5 nM) for the indicated times (a) or with various concentrations of FV variants for 20 minutes (b). FXa generation was initiated by the addition of FIXa (2 nM) and FX (200 nM) for 1 minute. The symbols used are as follows: open circles, WT; closed circles, W1920R; open squares, R506Q; closed squares, no FV. Values of FXa generation at the initial time (a) or in the absence of FV variants (b) were regarded as 100%. The data in (a) were fitted on an equation of single exponential decay (dashed lines). All experiments were performed at least 3 separate times, and the average values are shown. (B) A1 cleavage at Arg336; FVIII (10 nM) with PL (20 μM) was activated by thrombin (5 nM) for 30 second, followed by the addition of hirudin (2.5 U/mL). Generated FVIIIa was incubated with mixtures of APC (0.5 nM), PS (5 nM), and FV variants (0.5 nM) for the indicated times. Samples were analyzed on 8% gels, followed by western blotting using an anti-A1 C5 IgG, as described in "Materials and methods" (a). Band densities of intact $A1^{1-372}$ observed from panel a were measured by quantitative densitometry. Density before the addition of APC was regarded as 100% (b). The plotted data were fitted in an equation of single exponential decay (dashed lines). The symbols used are as follows: open circles, WT; closed circles, W1920R; open squares, R506Q. All experiments were performed at least 3 separate times, and the average values are shown.

Table 4. Kinetic parameters determined on FVIIIa inactivation by APC and PS in the presence of recombinant FV variants

FV variants	Rate constant: k, minutes^{-1} (-fold)	
	FVIIIa inactivation	Cleavage at Arg336
WT	0.742 ± 0.034 (1)	0.274 ± 0.034 (1)
W1920R	0.239 ± 0.021 (0.32)	Not determined
R506Q	0.390 ± 0.012 (0.53)	0.110 ± 0.076 (0.40)
None	0.246 ± 0.019 (0.33)	Not determined

Values were calculated by nonlinear least squares regression from the data shown in Figure 7A-B, using the single exponential decay.

most influential defect in the APCR mechanism. The complete loss of cleavage at Arg306 in FV_{Nara} also contributed to the stability of FVa:C. These findings provide potential new insights into the physiological role or roles of FV in (anti)coagulation systems.

The recurrence of DVT in FV_{Nara} was evident despite low levels of plasma FV:C. This observation appears to be unique in FV mutations reported with APCR. The precise reason or reasons for thrombotic symptoms in these circumstances remain to be clarified but could be explained by some laboratory features. First, moderately low levels of plasma FV:C (>5%) promote thrombin generation near to normal plasma and could facilitate significant effects on APCR. The thrombin-related procoagulant capacity of lower levels of FV:C (<2~3%) is very restricted, however, and the anticoagulant function of FV might be negligible. Second, platelet FV:C might be more important than plasma FV:C in physiological procoagulant activity.[39] Platelet FV:C in FV_{Nara} was ~20% (data not shown), and the peak level of thrombin formation in PRP was comparable to that of normal PRP (~90% of normal). The peak thrombin after the addition of APC was increased (145% of normal) (Figure 2Ab). Third, other hemostasis-related mechanisms may have a potential effect on the thrombotic diathesis. Other laboratory findings were within normal range in our patient, however, and we demonstrated directly that FV-W1920R conferred APCR.

The APCR mechanisms in FV_{Nara} appeared to be distinct from other APCR-associated FV mutations. With the exception of $FV_{Liverpool}$ (I359T),[40] all FV mutations have been identified in the HCh and constitute point mutations at cleavage sites that lead to the impairment of FV(a) inactivation. Delayed cleavage at Arg306 was described in $FV_{Liverpool}$, resulting in impaired inactivation of FVa and in clinically severe DVT. This mutation led to the creation of a glycosylation consensus sequence at Asn357 that is slightly remote from the Arg306 site. Cleavage at Arg506 in FVa and APC cofactor activity for FVIIIa inactivation was normal. However, W1920R is significantly remote from the APC-cleavage sites and from moderated cleavage at both Arg306 and Arg506. Although W1920 in FV is close to the PL-binding site,[36] the binding ability of W1920R to PL was almost equivalent to that of FV-WT, indicating that W1920R in FV_{Nara} might affect the direct association (binding-site) or indirect association (conformational change) with APC. In addition, W1920R was little cleaved by APC at Arg306, depending on PS, which might supporting a defective interaction with PS. Our conclusion that FV_{Nara} was resistant to APC inactivation through an impaired interaction with this protease might be further supported by observations that FVa-W1920R, when assembled into prothrombinase, was protected from FXa-catalyzed APC inactivation and that the inhibitory effect of FXa on APC-catalyzed inactivation of FVa-W1920R was observed, similar to WT (data not shown).

FV_{Leiden} is known to be a major cause of hereditary thrombotic diseases among Caucasians.[2,41] Studies of the ethnic distribution of FV_{Leiden} indicated that the mutation was not found in Asians.[17,18] A different FV mutation (E666D) causing APCR coupled with DVT has been reported in China,[42] but there are no reports of FV-associated APCR in Japan. The parents of the current propositus were heterozygous for the W1920R mutation, but they have not developed any thrombotic symptoms to date, although aPTT-based assays demonstrated mild APCR. It is possible that similar to FV_{Leiden}, the heterozygote FV_{Nara} may have a potential risk for thrombosis compounded by other prothrombotic factors.

Acknowledgments

We thank Dr Koji Yada, Dr Hiroaki Minami, and Dr Shoko Furukawa for the clinical support.

This work was partly supported by grants from Ministry of Education, Culture, Sports, Science and Technology (MEXT) Grants-in-Aid for Scientific Research (KAKENHI) (21591370 and 24591558 to K.N.) and an unrestricted research grant from Baxter (to K.F.).

Authorship

Contribution: K.N. and K.A. designed of research; K.N. and K.S. wrote the manuscript; K.N., K.S., K.O., and T.M. performed experiments; K.N., K.S., and K.O. analyzed the data; and K.F. and M.S. supervised the study, interpreted data, and edited the manuscript.

Conflict-of-interest disclosure: K.S. is an endowed assistant professor funded by Baxter; has given lectures at educational symposiums organized by Baxter, Bayer, and Novo Nordisk; has received payment for lectures from Baxter, Bayer, and Novo Nordisk; and has received the Award from Baxter Coagulation Research Fund in Japan. K.F. and K.A. are professors of additional post in Molecular Genetics of Coagulation Disorder without additional salary. K.A. is a board member of the Factor Eight Inhibitor Bypass Activity Post Marketing Surveillance Study Board in Japan organized by Baxter; has received payment for lectures from Baxter, Bayer, Biogen Idec, Kaketsuken, Novo Nordisk, and Pfizer; has received payment for consultancy meetings with Baxter, Bayer, CSL Behring, Kaketsuken, Novo Nordisk, and Pfizer; and has received unrestricted grants supporting research from Pfizer. K.F. is an investigator of Hemophilia Research Study Update organized by Baxter, a board member of the Advate Safety Board in Japan organized by Baxter, and a board member of the Benefix Post Marketing Surveillance Study Board in Japan, organized by Pfizer; has received payment for consultancy meetings with Baxter, Pfizer, Biogen Idec, Bayer, CSL Behring, Kaketsuken, SRL, Mitsubishi Chemical Medience, and Novo Nordisk; has received unrestricted grants supporting research from Baxter, Pfizer, Bayer, Kaketsuken, Japan Blood Products Organization, and CSL Behring; and has received payment for lectures from Baxter, Bayer, Pfizer, Novo Nordisk, CSL Behring, Roche Diagnostics, Fujirebio Inc, and Sekisui Medical. M.S. is a board member of the Feiba and an Advate Safety Board in Japan, organized by Baxter, and a board member of the Benefix Post Marketing Surveillance Study Board in Japan, organized by Pfizer; has received payment for consultancy meetings with Baxter, Pfizer, Biogen Idec, Bayer, CSL Behring, Kaketsuken, Chugai Therapeutic Company, and Novo Nordisk; has received unrestricted grants supporting research from Baxter, Pfizer, Bayer, Kaketsuken, Novo Nordisk, Chugai

Pharmaceutical Company, and CSL Behring; and has received payment for lectures from Baxter, Bayer, Novo Nordisk, and Pfizer. The remaining authors declare no competing financial interests.

Correspondence: Keiji Nogami, Department of Pediatrics, Nara Medical University, Kashihara, Nara 634-8522, Japan; e-mail: roc-noga@naramed-u.ac.jp.

References

1. Dahlbäck B, Carlsson M, Svensson PJ. Familial thrombophilia due to a previously unrecognized mechanism characterized by poor anticoagulant response to activated protein C: prediction of a cofactor to activated protein C. *Proc Natl Acad Sci USA.* 1993;90(3):1004-1008.
2. Bertina RM, Koeleman BP, Koster T, et al. Mutation in blood coagulation factor V associated with resistance to activated protein C. *Nature.* 1994;369(6475):64-67.
3. Rosing J, Tans G. Coagulation factor V: an old star shines again. *Thromb Haemost.* 1997;78(1): 427-433.
4. Suzuki K, Dahlbäck B, Stenflo J. Thrombin-catalyzed activation of human coagulation factor V. *J Biol Chem.* 1982;257(11):6556-6564.
5. Foster WB, Nesheim ME, Mann KG. The factor Xa-catalyzed activation of factor V. *J Biol Chem.* 1983;258(22):13970-13977.
6. Walker FJ, Sexton PW, Esmon CT. The inhibition of blood coagulation by activated Protein C through the selective inactivation of activated Factor V. *Biochim Biophys Acta.* 1979;571(2): 333-342.
7. Suzuki K, Stenflo J, Dahlbäck B, Teodorsson B. Inactivation of human coagulation factor V by activated protein C. *J Biol Chem.* 1983;258(3): 1914-1920.
8. Nicolaes GA, Tans G, Thomassen MC, et al. Peptide bond cleavages and loss of functional activity during inactivation of factor Va and factor VaR506Q by activated protein C. *J Biol Chem.* 1995;270(36):21158-21166.
9. Gale AJ, Xu X, Pellequer JL, Getzoff ED, Griffin JH. Interdomain engineered disulfide bond permitting elucidation of mechanisms of inactivation of coagulation factor Va by activated protein C. *Protein Sci.* 2002;11(9):2091-2101.
10. Mann KG, Nesheim ME, Church WR, Haley P, Krishnaswamy S. Surface-dependent reactions of the vitamin K-dependent enzyme complexes. *Blood.* 1990;76(1):1-16.
11. Eaton D, Rodriguez H, Vehar GA. Proteolytic processing of human factor VIII. Correlation of specific cleavages by thrombin, factor Xa, and activated protein C with activation and inactivation of factor VIII coagulant activity. *Biochemistry.* 1986;25(2):505-512.
12. Fay PJ, Smudzin TM, Walker FJ. Activated protein C-catalyzed inactivation of human factor VIII and factor VIIIa. Identification of cleavage sites and correlation of proteolysis with cofactor activity. *J Biol Chem.* 1991;266(30):20139-20145.
13. Gale AJ, Cramer TJ, Rozenshteyn D, Cruz JR. Detailed mechanisms of the inactivation of factor VIIIa by activated protein C in the presence of its cofactors, protein S and factor V. *J Biol Chem.* 2008;283(24):16355-16362.
14. O'Brien LM, Mastri M, Fay PJ. Regulation of factor VIIIa by human activated protein C and protein S: inactivation of cofactor in the intrinsic factor Xase. *Blood.* 2000;95(5):1714-1720.
15. Thorelli E, Kaufman RJ, Dahlbäck B. The C-terminal region of the factor V B-domain is crucial for the anticoagulant activity of factor V. *J Biol Chem.* 1998;273(26):16140-16145.
16. Lu D, Kalafatis M, Mann KG, Long GL. Comparison of activated protein C/protein S-mediated inactivation of human factor VIII and factor V. *Blood.* 1996;87(11):4708-4717.
17. Rees DC, Cox M, Clegg JB. World distribution of factor V Leiden. *Lancet.* 1995;346(8983): 1133-1134.
18. Rees DC. The population genetics of factor V Leiden (Arg506Gln). *Br J Haematol.* 1996;95(4): 579-586.
19. Williamson D, Brown K, Luddington R, Baglin C, Baglin T. Factor V Cambridge: a new mutation (Arg306—>Thr) associated with resistance to activated protein C. *Blood.* 1998;91(4): 1140-1144.
20. Norstrøm E, Thorelli E, Dahlbäck B. Functional characterization of recombinant FV Hong Kong and FV Cambridge. *Blood.* 2002;100(2):524-530.
21. Chan WP, Lee CK, Kwong YL, Lam CK, Liang R. A novel mutation of Arg306 of factor V gene in Hong Kong Chinese. *Blood.* 1998;91(4): 1135-1139.
22. Nicolaes GA, Dahlbäck B. Factor V and thrombotic disease: description of a janus-faced protein. *Arterioscler Thromb Vasc Biol.* 2002; 22(4):530-538.
23. Foster PA, Fulcher CA, Houghten RA, de Graaf Mahoney S, Zimmerman TS. Localization of the binding regions of a murine monoclonal anti-factor VIII antibody and a human anti-factor VIII alloantibody, both of which inhibit factor VIII procoagulant activity, to amino acid residues threonine351-serine365 of the factor VIII heavy chain. *J Clin Invest.* 1988;82(1):123-128.
24. Mimms LT, Zampighi G, Nozaki Y, Tanford C, Reynolds JA. Phospholipid vesicle formation and transmembrane protein incorporation using octyl glucoside. *Biochemistry.* 1981;20(4):833-840.
25. Shinozawa K, Amano K, Suzuki T, et al. Molecular characterization of 3 factor V mutations, R2174L, V1813M, and a 5-bp deletion, that cause factor V deficiency. *Int J Hematol.* 2007;86(5):407-413.
26. Matsumoto T, Nogami K, Ogiwara K, Shima M. A modified thrombin generation test for investigating very low levels of factor VIII activity in hemophilia A. *Int J Hematol.* 2009;90(5):576-582.
27. Castoldi E, Brugge JM, Nicolaes GA, Girelli D, Tans G, Rosing J. Impaired APC cofactor activity of factor V plays a major role in the APC resistance associated with the factor V Leiden (R506Q) and R2 (H1299R) mutations. *Blood.* 2004;103(11):4173-4179.
28. Ortel TL, Devore-Carter D, Quinn-Allen M, Kane WH. Deletion analysis of recombinant human factor V. Evidence for a phosphatidylserine binding site in the second C-type domain. *J Biol Chem.* 1992;267(6):4189-4198.
29. Shen L, Dahlbäck B. Factor V and protein S as synergistic cofactors to activated protein C in degradation of factor VIIIa. *J Biol Chem.* 1994; 269(29):18735-18738.
30. Nogami K, Wakabayashi H, Schmidt K, Fay PJ. Altered interactions between the A1 and A2 subunits of factor VIIIa following cleavage of A1 subunit by factor Xa. *J Biol Chem.* 2003;278(3): 1634-1641.
31. Kamikura Y, Wada H, Yamada A, et al. Increased tissue factor pathway inhibitor in patients with acute myocardial infarction. *Am J Hematol.* 1997; 55(4):183-187.
32. Kalafatis M, Bertina RM, Rand MD, Mann KG. Characterization of the molecular defect in factor VR506Q. *J Biol Chem.* 1995;270(8):4053-4057.
33. Thorelli E, Kaufman RJ, Dahlbäck B. Cleavage of factor V at Arg 506 by activated protein C and the expression of anticoagulant activity of factor V. *Blood.* 1999;93(8):2552-2558.
34. Macedo-Ribeiro S, Bode W, Huber R, et al. Crystal structures of the membrane-binding C2 domain of human coagulation factor V. *Nature.* 1999;402(6760):434-439.
35. Saleh M, Peng W, Quinn-Allen MA, et al. The factor V C1 domain is involved in membrane binding: identification of functionally important amino acid residues within the C1 domain of factor V using alanine scanning mutagenesis. *Thromb Haemost.* 2004;91(1):16-27.
36. Adams TE, Hockin MF, Mann KG, Everse SJ. The crystal structure of activated protein C-inactivated bovine factor Va: Implications for cofactor function. *Proc Natl Acad Sci USA.* 2004;101(24): 8918-8923.
37. Fay PJ. Activation of factor VIII and mechanisms of cofactor action. *Blood Rev.* 2004;18(1):1-15.
38. Nogami K, Wakabayashi H, Fay PJ. Mechanisms of factor Xa-catalyzed cleavage of the factor VIIIa A1 subunit resulting in cofactor inactivation. *J Biol Chem.* 2003;278(19):16502-16509.
39. Duckers C, Simioni P, Spiezia L, et al. Residual platelet factor V ensures thrombin generation in patients with severe congenital factor V deficiency and mild bleeding symptoms. *Blood.* 2010;115(4): 879-886.
40. Mumford AD, McVey JH, Morse CV, et al. Factor V I359T: a novel mutation associated with thrombosis and resistance to activated protein C. *Br J Haematol.* 2003;123(3):496-501.
41. Zöller B, Svensson PJ, He X, Dahlbäck B. Identification of the same factor V gene mutation in 47 out of 50 thrombosis-prone families with inherited resistance to activated protein C. *J Clin Invest.* 1994;94(6):2521-2524.
42. Cai H, Hua B, Fan L, Wang Q, Wang S, Zhao Y. A novel mutation (g2172—>c) in the factor v gene in a chinese family with hereditary activated protein C resistance. *Thromb Res.* 2010;125(6): 545-548.

Journal of Thrombosis and Haemostasis, **12**: 1503–1512 DOI: 10.1111/jth.12660

ORIGINAL ARTICLE

Coagulation function and mechanisms in various clinical phenotypes of patients with acquired factor V inhibitors

T. MATSUMOTO, K. NOGAMI and M. SHIMA
Department of Pediatrics, Nara Medical University, Kashihara, Japan

To cite this article: Matsumoto T, Nogami K, Shima M. Coagulation function and mechanisms in various clinical phenotypes of patients with acquired factor V inhibitors. *J Thromb Haemost* 2014; **12**: 1503–12.

Summary. *Background:* The clinical phenotype of individuals with acquired factor V (A-FV) inhibitors varies from asymptomatic (non-B group) to life-threatening bleeding (B group), but the mechanism(s) underlying this variation in hemorrhagic phenotype are poorly understood. *Objective:* To investigate coagulation mechanistically in a range of patients with A-FV antibodies. *Methods and Results:* Ten cases of A-FV inhibitors in the non-B ($n = 5$) and B groups ($n = 5$) were studied. Thrombin generation assays in these plasmas revealed little thrombin generation, despite similar FV activity levels in both groups. However, prothrombin time-based clot waveform analysis revealed that the clot times were significantly prolonged and the maximum velocity and acceleration of coagulation were lower in the B group than in the non-B group, suggesting that this technique might be useful for predicting and monitoring hemorrhagic symptoms. A-FV inhibitors from the non-B group recognized predominantly the FV heavy chain, whereas those from the B group recognized the light chain. Purified anti-FV autoantibodies (autoAbs) from the B group inhibited FV binding to phospholipid by 60–90%, whereas there was little effect on this reaction in the non-B group. In addition, anti-FV autoAbs from the non-B group impaired the activated protein C (APC) cofactor activity of FV in FVIIIa inactivation mechanisms, and delayed APC-catalyzed cleavage of FVa at Arg306, but not at Arg506, indicating the presence of APC resistance in the non-B group. *Conclusions:* The results suggest that the different hemorrhagic phenotypes in A-FV inhibitors depend on the specific epitope of anti-FV autoAbs, and appear to be associated with an imbalance of procoagulant and anticoagulant function.

Keywords: APC resistance; blood coagulation factor inhibitors; clinical laboratory techniques; factor V; hemostatic techniques.

Correspondence: Keiji Nogami, Department of Pediatrics, Nara Medical University, 840 Shijo-cho, Kashihara, Nara 634-8522, Japan.
Tel.: +81 744 29 8881; fax +81 744 24 9222.
E-mail: roc-noga@naramed-u.ac.jp

Received 11 April 2014
Manuscript handled by: R. Camire
Final decision: P. H. Reitsma, 13 June 2014

© 2014 International Society on Thrombosis and Haemostasis

Introduction

Factor V is a single-chain molecule consisting of 2196 amino acids arranged in six domains, A1–A2–B–A3–C1–C2 [1,2]. FV governs the balance of coagulation by regulating opposing functional mechanisms. The procoagulant action of FV is associated with cofactor activity for FXa in the prothrombinase complex, which catalyzes the conversion of prothrombin to thrombin on a phospholipid (PL) surface [3]. Thrombin proteolyses FV, generating the activated form (FVa), a heterodimer composed of a 105-kDa heavy chain (HCh), containing the A1 and A2 domains, and 71/74-kDa light chain (LCh), containing the A3, C1 and C2 domains. The development of a hypercoagulant state is controlled, however, by downregulation of cofactor activity by activated protein C (APC) with protein S (PS). FVa is rapidly inactivated by proteolytic cleavage at Arg506, and then at Arg306 and Arg679 [4]. Cleavage at Arg506 is essential for the exposure of other cleavage sites, but is unlikely to contribute significantly to the reduction in activity. Cleavage at Arg306 results in almost complete loss of FVa activity (FVa:C), but that at Arg679 has a more modest impact [5]. Irregularities in the mechanism of APC-mediated inactivation of FVa are therefore associated with thrombotic episodes in the presence of sustained prothrombin activation.

An alternative function of FV is an as anticoagulant cofactor of APC in the inactivation of FVIIIa [6]. FVIIIa is inactivated by cleavage at Arg336 by APC [7,8]. In the process of APC-mediated inactivation of FVIIIa, FV functions as an anticoagulant cofactor of APC, resulting in acceleration of FVIIIa inactivation [9]. This anticoagulant activity of FV is mediated by a product of proteoly-

sis by APC, prior to cleavage by thrombin. Cleavage at Arg506 of FV attached to the B domain is essential for the anticoagulant FV activity, whereas cleavage at Arg306 appears to be unlikely to contribute to this mechanism [9–12]. Any molecular defect of these cleavage reactions confers APC resistance (APCR). Clinically, individuals with the Arg506Gln mutation (FV Leiden) have a poor anticoagulant response to APC, which is associated with a significant increase in the risk of deep vein thrombosis (DVT) [13,14].

Acquired FV (A-FV) inhibitors occur rarely, but may develop spontaneously as autoantibodies (autoAbs) in previously normal individuals, after exposure to topical hemostatic agents containing bovine thrombin, antibiotic administration, cancer, and autoimmune disorders [15–18]. These anti-FV autoAbs are frequently associated with hemorrhagic symptoms, which are usually mild but are occasionally severe. Some patients remain asymptomatic, however, and hemorrhagic symptoms appear to be limited in ~ 20% of patients diagnosed with A-FV inhibitors [17,18]. It is of note that only four patients with A-FV inhibitors have presented with thrombotic manifestations [18]. Among these cases with DVT, Kalafatis *et al.* reported that the anti-FV autoAbs from one individual diminished both APC-mediated FVa inactivation and FV cofactor activity in APC-mediated FVIIIa inactivation, reflecting APCR [19]. Thrombotic mechanism(s) in other three cases appear not to have been explored, however. Moreover, the precise reasons for the variation in hemorrhagic phenotype in patients with A-FV inhibitors are poorly understood. We therefore investigated coagulation mechanisms in a range of patients with A-FV inhibitors, using a combination of established functional techniques.

Materials and methods

Reagents

Recombinant FVIII was a generous gift from Bayer (Osaka, Japan). Purified FV/FVa, FIXa, FX/FXa, prothrombin, α-thrombin, APC, PS, 5-dimethylamino-naphthalene-1-sulfonylarginine-*N*-(3-ethyl-1,5-pentanediyl)-amide (DAPA) and anti-FV HCh and LCh mAbs, AHV-5146 and AHV-5112, respectively (Hematologic Technologies, Essex Junction, VT, USA), hirudin (Calbiochem, San Diego, CA, USA) and chromogenic substrates S-2222 and S-2238 (Chromogenix, Milano, Italy) were commercially purchased. The activated partial thromboplastin time (APTT) and prothrombin time (PT) reagents, ellagic acid (Sysmex, Kobe, Japan), FV-deficient plasma (George King Biomedical, Overland Park, KS, USA), lipidated tissue factor (Innovin, Dade Behring, Marburg, Germany) and the thrombin substrate Z-Gly-Gly-Arg-AMC (Bachem, Bubendorf, Switzerland) were purchased. PL vesicles (phosphatidylserine/phosphatidylcholine/phosphatidylethanolamine; 10% : 60% : 30%) were prepared with *N*-octylglucoside [20]. HBS buffer (20 mM Hepes, pH 7.2, 0.1 M NaCl, 0.01% Tween-20) containing 2.5 mM $CaCl_2$ was used for dilution.

Blood samples

Whole blood was obtained by venepuncture from patients into tubes containing a 1 : 9 volume of 3.8% (w/v) trisodium citrate. Platelet-poor plasma was recovered after centrifugation of citrated whole blood for 10 min at 1500 × *g*. Normal pooled plasmas were prepared from 30 normal healthy individuals (25 : 5 male/female). All plasmas were stored at − 80 °C and thawed at 37 °C immediately prior to the assays. All samples were obtained after informed consent had been obtained, following local ethical guidelines.

FV activity (FV:C), FV antigen (FV:Ag) and FV inhibitor levels

FV:C and FV:Ag were measured with PT-based clotting assays with FV-deficient plasma and with ELISAs, respectively. A-FV inhibitor titers were determined with the Bethesda method described for FVIII antibodies [21].

Anti-FV inhibitor autoAbs

Anti-FV IgGs were purified from the plasma of patients with A-FV inhibitors. IgG preparations were fractionated by affinity chromatography on protein G–Sepharose. F $(ab')_2$ fragments were prepared by the use of immobilized pepsin–Sepharose (Pierce, Rockford, IL, USA). Specific regions of FV/FVa recognized by these antibodies were determined with SDS-PAGE and western blotting. The binding of FV/FVa fragments to anti-FV autoAbs was detected by the addition of anti-human peroxidase-linked antibody. The effects of FV inhibitors were expressed as a function of IgG concentration in this study, although the percentage of anti-FV in IgG preparations varied between patients.

Clot waveform analysis (CWA)

PT and APTT measurements were performed with the MDA-II Hemostasis System (Tcoag Ireland, Bray, Ireland). The clot waveforms obtained were computer-processed with the commercial kinetic algorithm [22]. The minimum value of the first derivative (min1) was calculated as an indicator of the maximum velocity of coagulation achieved. The minimum value of the second derivative (min2) was calculated as an indicator of the maximum acceleration of the reaction achieved. As the minima of min1 and min2 are derived from negative changes, the data were expressed as min1 and min2. The

© 2014 International Society on Thrombosis and Haemostasis

clot time was defined as the time until the start of coagulation.

Prothrombinase assay

The rate of conversion of prothrombin to thrombin was monitored in a purified system. FVa (2 nM) was incubated with various concentrations of anti-FV autoAbs at 37 °C for 30 min. The reactants were mixed with prothrombin (1.4 μM), PL (20 μM), and DAPA (30 μM), and this was followed by initiation of the addition of FXa (10 pM). Aliquots were removed at appropriate times to assess the initial rates of product formation, and were mixed with EDTA (final concentration of 50 mM) to quench the reactions. Rates of thrombin generation were determined at an absorbance of 405 nm after the addition of S-2238 (final concentration of 0.46 mM). Thrombin generation was quantified from a standard curve prepared with known amounts of thrombin.

FV–PL binding assay

Binding of FV to immobilized PL was examined in a solid-phase based ELISA [23]. α-Phosphatidyl-L-serine (5 μg mL^{-1}) in methanol was added to microtiter wells and air-dried at 4 °C overnight. After washing of the wells, the wells were blocked by the addition of gelatin solution (5 mg mL^{-1}) at 37 °C for 2 h. FV (1 nM) and anti-FV autoAbs were incubated for 2 h. After washing, the mixture reactants were added to the PL-coated well, and incubated for 2 h. Bound FV was quantified by the addition of the anti-FV mAb AHV-5146 (2.5 μg mL^{-1}), followed by a goat anti-mouse peroxidase-linked antibody (3 μg mL^{-1}) and *O*-phenylenediamine dihydrochloride substrate. Reactions were quenched by the addition of 2 M H_2SO_4, and absorbance at 492 nm was measured. The amount of non-specific IgG binding without FV was < 3% of the total signal. Specific binding was estimated by subtracting the amount of non-specific binding.

APCR assays

Chromogenic assay FXa generation in plasma samples was performed with the COATEST SP FVIII assay (Chromogenix). The test specifically quantifies FVIIIa activity in 16-fold-diluted plasma, by measuring intrinsic FXa generation mediated by excess exogenous FIXa and FX with PL and $CaCl_2$. The simultaneous addition of APC (40 nM) with the cofactors PS and FV contained in plasma inhibits intrinsic FXa generation by inactivating FVIIIa. The APC sensitivity ratio (APCsr) was expressed as the absorbance in the absence of APC divided by that in its presence. A low APCsr value indicates a defect in the inactivation of FVIIIa, reflecting the APCR.

APC cofactor activity of FV The APC cofactor activity of FV was measured with an FVIIIa degradation assay, as previously reported, with minor modifications [9]. FVIII (10 nM) and PL (20 μM) were activated by thrombin (5 nM) for 30 s, and the reaction was terminated by the addition of hirudin (2.5 U mL^{-1}). The generated FVIIIa was then incubated for 7 min with APC (0.5 nM), PS (5 nM), and the mixtures of FV (1 nM) and the indicated amounts of anti-FV autoAbs or normal IgG. The mixture was 10-fold-diluted prior to incubation with FIXa (2 nM) and FX (200 nM) for 1 min. After the addition of EDTA, generated FXa was evaluated by the use of S-2222 at 405 nm. Control experiments were performed without either APC or FV. FXa generation was quantified from a standard curve prepared with known amounts of FXa.

APC-catalyzed cleavage of FVa FV (8 nM) and anti-FV autoAbs (30 μg mL^{-1}) were incubated for 2 h at 37 °C. The mixtures were incubated with thrombin (30 nM) for 5 min at 37 °C, and the thrombin reaction was rapidly terminated by the addition of hirudin (10 U mL^{-1}). Samples containing the generated FVa (2 nM) were incubated with PL (20 μM), PS (30 nM), and APC (0.7 nM). Aliquots were removed from the mixtures at the indicated times, and reactions were immediately terminated by adding SDS and boiling for 3 min.

Western blot analysis

SDS-PAGE was performed with 8% gels, and this was followed by western blotting [24]. Protein bands were probed with the indicated anti-FV mAb, and this was followed by the addition of goat anti-mouse peroxidase-linked antibody. Signals were detected with enhanced chemiluminescence (PerkinElmer Life Science, Boston, MA, USA). Densitometric scans were quantified with IMAGEJ 1.34 (NIH, Bethesda, MD, USA).

Results

Global coagulation function in plasmas from patients with A-FV inhibitors

The properties of five patients with A-FV inhibitors in the asymptomatic group (non-B group) and five patients with severe bleeding symptoms (B group) are summarized in Table 1. To define the bleeding symptoms, we used the Vicenza Bleeding Score [25] to evaluate hemorrhage. In the B group, the scores ranged from 3 to 7, whereas in the non-B group the scores were 0. In both groups, both the PT and the APTT were markedly prolonged, and FV:C ranged from undetectable to low levels (~ 10 IU dL^{-1}), showing that the routine clotting tests and FV:C levels did not well reflect the clinical phenotype. FV:Ag levels

© 2014 International Society on Thrombosis and Haemostasis

Table 1 Properties of patients' plasmas with acquired factor V inhibitors

Case	Sex	PT (s)	APTT (s)	FV:C (IU dL^{-1})	FV:Ag (IU dL^{-1})	Inhibitor titer (BU mL^{-1})	Ig subtype	Bleeding score*	Underlying disease
Asymptomatic (non-B group)									
1	M	53.5	> 150	2.3	93.8	4.3	IgG	0	Chronic thyroiditis
2	M	47.4	133	11.5	86.3	5.4	IgG	0	Progressive supranuclear palsy
3	M	67.7	> 150	< 1.0	137	11.8	IgG	0	Intraductal papillary mucinous tumor of pancreas
4	M	83.6	> 150	< 1.0	180	1.7	IgG	0	Atrial fibrillation
5	F	34.1	66.8	1.7	55.6	8.7	IgG	0	None
Severe bleeding (B group)									
6	M	94.5	> 150	8.0	81.3	118	IgG	4	Aspiration pneumonia, asthma
7	F	56.0	> 150	< 1.0	75.0	16	IgG	4	Surgery for valve replacement (TR, AS, MR)
8	M	> 100	> 150	< 1.0	57.8	64	IgG	3	Chronic renal failure
9	M	> 100	> 150	< 1.0	2.1	9.9	IgG	5	None
10	M	81.1	92.3	< 1.0	36.2	8.2	IgG	7	None
Control	–	12.1	30.3	–	–	–	–	–	–

APTT, activated partial thromboplastin time; AS, aortic stenosis; F, female; FV:Ag, FV antigen; FV:C, FV activity; M, male; MR, mitral regurgitation; PT, prothrombin time; TR, tricuspid regurgitation. *Numbers represent the bleeding score calculated according to Rodeghiero *et al.* [25].

(except for case 9) were not significantly different between groups, supporting the contention that low FV:C in patients was attributable to functional inhibition by A-FV inhibitors. FV inhibitor titers were 6.4 ± 3.9 and 43 ± 48 BU mL^{-1} in the non-B group and B group, respectively. The immunoglobulin class was IgG in all patients, and none had been exposed to antibiotic therapy or bovine thrombin products. In all cases, platelet counts, other coagulation proteins, anticoagulant proteins (protein C [PC]/PS, antithrombin) and fibrinolytic proteins showed normal plasma levels. No autoAbs, except for those against FV, were detectable (data not shown). These findings typified the difficulties in identifying the different clinical phenotypes on the basis of basic coagulation tests.

We compared the different inhibitor groups by using the following global coagulation assays: the thrombin generation test (TGT) and CWA. There was little evident thrombin generation in patient plasmas, even after 60 min of reaction time (data not shown), suggesting that evaluation of the different A-FV inhibitors with this technique was not informative. Unlike the TGT, CWA reflects the process of fibrin formation. Representative curves of the PT-based CWA are shown in Fig. 1 (upper). Because of the small sample volume from case 7, this case failed to show the clot waveform. The clot time observed in the non-B group was markedly shorter that that in the B group (56.5 ± 19.6 vs. 104 ± 20 s, $P = 0.0044$) (Fig. 1A), and the parameters min1 and min2 were significantly greater in the non-B group than in the B group (min1, 3.09 ± 1.00 vs. 0.87 ± 0.32, $P = 0.0022$; min2, 0.90 ± 0.48 vs. 0.15 ± 0.06, $P = 0.009$) (Fig. 1B,C). These findings appeared to be in keeping with the contrasting hemorrhagic symptoms observed in the different patients. The data suggested that CWA might be a useful method for predicting and monitoring the bleeding tendency in patients with A-FV inhibitors.

Binding epitope(s) of A-FV inhibitors

To clarify the precise mechanism(s) involved in the distinct phenotypes in patients with A-FV inhibitors, we initially attempted to determine the FV epitopes of the antibodies by immunoblotting. Figure 2 shows that, in the non-B group, three inhibitors reacted with the HCh alone. In contrast, in the B group, two inhibitors reacted with the LCh alone, and two inhibitors reacted with both chains. The results suggested the possible presence of distinct epitopes of anti-FV autoAbs between both groups. The reason for the presence of some bands in FV lanes (cases 1 and 10) was unclear, but partially proteolysed FV may be a contaminant of the single-chain FV preparation. Binding to FV(a) fragments was not observed in two cases from the non-B group and in one case from the B group. This may be attributable to weak binding reactivity of individual inhibitors and/or to low sensitivity of this assay.

Effects of purified anti-FV autoAbs on FV–PL binding

The specific properties of A-FV inhibitors were further examined with immune-purified IgGs from the patients' plasmas. With mixtures of normal plasma and purified anti-FV IgG, all CWA parameters were similar to those obtained with native patients' plasmas (data not shown), confirming that the defective coagulation function in both groups was attributable to the presence of antibody. The LCh of FV, and in particular the C2 domain, contains PL-binding site(s) [26]. The effects of purified anti-FV autoAbs on FV binding to immobilized PL were therefore examined with a solid-phase-based ELISA. All IgGs from

© 2014 International Society on Thrombosis and Haemostasis